

Characterizing Structure, Defects, and Chemistry

CHAPTER PREVIEW

In this chapter we will discuss techniques that can produce useful information about the structure, chemistry, and bonding in ceramics. There are so many characterization methods available that books are written on each one. Since we cannot cover all the details or even all the techniques, we will give examples and aim at making you aware of the key ones and their applications.

We can group the techniques into six categories:

- Imaging using visible (or nearly visible) light
- Imaging using electrons [mainly scanning electron microscopy (SEM) and transmission electron microscopy (TEM)]
- Imaging using sensing [atomic force microscopy (AFM) and other scanned probes that “sense” a force or field]
- Scattering and diffraction (using X-rays, neutrons, α -particles, electrons)
- Spectroscopy and spectrometry [using X-rays for energy dispersive spectrometry (EDS) and wavelength dispersive spectroscopy (WDS), Raman, infrared (IR), etc.]
- Thermal analysis (measuring changes, e.g., enthalpy, as a function of temperature)

Most of the techniques we describe can be used to study other classes of materials, but our examples will all be related to ceramics.

The suitability of a characterization technique depends on the type of information we hope to obtain and may also be dictated by the size of our sample, what part of the sample is important, and whether we can destroy the sample. There are some limitations:

- Reflection techniques examine only surfaces.
- Techniques using electrons require the sample to be in a vacuum.
- Techniques using transmitted electrons generally require the sample to be thin.
- For nanomaterials we need high resolution.

We always ask two questions:

- How much material is required for the analysis?
- Is it destructive or nondestructive?

For example, TEM is invariably destructive, but you need a very small amount of material for the analysis.

10.1 CHARACTERIZING CERAMICS

In characterizing a ceramic, whether it is a single crystal, polycrystalline, or a glass, there are certain types of information that we are interested in obtaining:

- Chemistry. What is the composition, how does it vary within the sample, etc.?
- Structure. Is the ceramic crystalline or glass or a mixture of the two? What polymorph is present?
- Microstructure. Is the structure the same throughout the sample? Polycrystalline ceramics cannot be uniform. Even glass can be structurally inhomogeneous.
- Surface. Whether the sample is crystalline or not, the nature of the surface is often particularly important. If the sample is crystalline then surface orientation may

TABLE 10.1 Summary of Tools for Ceramics Using Chemical and Physical Characteristics

<i>Chemical characteristic</i>	<i>Characterization tool</i>
Composition	X-ray diffraction (XRD) X-ray fluorescence (XRF) Neutron activation analysis (NAA) Mass spectrometry (Mass Spec)
Elemental distribution/local chemistry	Scanning electron microscope (SEM) with X-ray energy-dispersive spectroscopy (XEDS) Electron probe microanalysis (EPMA) Transmission electron microscopy (TEM) with XEDS TEM with electron energy-loss spectroscopy (EELS)
Surface/interface chemistry	X-ray photoelectron spectroscopy (XPS, ESCA) Auger electron spectroscopy (AES) Secondary ion mass spectroscopy (SIMS) Rutherford backscattering spectrometry (RBS) Ultraviolet photoelectron spectroscopy (UPS) Infrared (IR) spectroscopy Raman spectroscopy
Phase changes (e.g., decomposition and dehydration)	Thermomechanical analysis (TMA) Thermogravimetric analysis (TGA) Differential thermal analysis (DTA) Differential scanning calorimetry (DSC) Mass Spec (MS) <i>In situ</i> XRD
Surface area/porosity (see Chapter 20)	Small-angle neutron scattering (SANS) Small-angle X-ray scattering (SAXS) Mercury porosimetry
Density homogeneity	VLM SEM X-ray radiography/CT scan Ultrasound Die penetration
Particle/grain size, distribution, morphology, and texture	VLM and quantitative stereology SEM and quantitative stereology Electron backscattering spectroscopy (EBSD) TEM XRD
Phase identification/molecular structure	XRD EBSD FTIR Raman spectroscopy EXAFS Neutron diffraction Mössbauer spectroscopy Nuclear magnetic resonance
(NMR) Phase transitions: e.g., structural transformations	DTA DSC TMA <i>In situ</i> XRD

be critical. Even the surface of a glass will be different chemically and structurally from the bulk. In nanomaterials the surface is the most important feature, since most of the atoms are there.

- Defects. In crystals we often want to determine dislocation density. In both crystals and glass we may be interested in the nature, concentration, and distribution of point defects. Techniques for characterizing defects are dealt with mainly in their respective chapters.

What we want to know determines which technique we should use. In the following sections our approach is to illustrate the type of information that can be obtained. Most of these methods are applicable not only to ceramics but to other classes of material. However, there are certain special features associated with ceramics:

- Techniques using electrons can be complicated because many ceramics charge locally, thus deflecting an electron beam.
- We are often interested in what happens while ceramics are being processed. Because of the environment or the high temperatures involved, such *in situ* studies may not be possible with the desired resolution.
- Ceramics are often multicomponent systems; knowing the average composition may not be too useful. So we may need local compositional analysis on a scale that may be in the nanometer range.
- Many ceramics contain light elements (e.g., B, C, N, O), which can be difficult to quantify.
- If we are interested in interfaces, for example, the interface may facet over short (<100 nm) distances and it may contain steps that are only nanometers high. In studying such interfaces, it is essential that both grains be observed, so that techniques requiring the sample to be broken along the interface would not be ideal (though they may be necessary).

Table 10.1 lists some of the techniques that you might consider to obtain specific information about your material. In most cases the use of a particular technique depends in part on its availability, and often a combination of techniques is necessary to get the complete picture.

10.2 IMAGING USING VISIBLE-LIGHT, IR, AND UV

Light interacts with the specimen in many ways; we then study the resulting image contrast. Contrast is produced by reflection, absorption, refraction, polarization, fluorescence, or diffraction. This contrast can be modified by physically changing the optical components and illumination mode of the microscope. The final image can also be processed, now mainly using computer techniques.

Visible-light microscopy (VLM) is used routinely for all ceramics. It is often referred to as optical microscopy, but essentially all microscopy is optical. The magnification of a VLM can range from 10× (a magnifying glass) to 50k× using a liquid between the specimen and the lens. Modern VLMs are equipped with digital cameras (video or still) and feed straight into the computer. Ceramics are often transparent, especially (but not necessarily) if they are glass, so we can then use reflected or transmitted light. The sample can be viewed supported on a table or inverted. The inverted microscope has some advantages, in particular, you can attach contacts to, indent into, or support liquids on the free surface. You also have more flexibility with the lighting.

The lateral resolution using VLM is about 250 nm and the depth of field has a similar value. Because of the poor depth of field of the VLM we often examine polished surfaces (as in metallography). Vertical resolution can be less than 1 nm using interference contrast, and this is bettered only by the scanned probe techniques.

Visible-light microscopy is usually available in every laboratory. While a conventional VLM may cost only \$2000, the best metallographic microscopes can cost >\$100k. There are numerous imaging methods used in VLM so we list only a few here:

Dark-field. The image is formed using only scattered light (if there is no specimen present then the image is dark). It is widely used in mineralogy where multiphase materials are common.

Polarized light. Polarized VLM distinguishes between isotropic and anisotropic materials and provides information on absorption color and boundaries between minerals of differing refractive indices. The technique provides local information on the structure and composition of materials as shown in Figure 10.1, which is an image of a neodymium-doped yttrium orthovanadate laser crystal. Individual grains, separated by low-angle grain boundaries, are clearly revealed by polarized VLM.

Nomarski (differential interference contrast). The idea here is that we use interference. Contrast is generated by phase differences between two rays (a sample ray and a reference ray). In the Nomarski microscope the two rays are created after the light has passed through the sample, where path differences occur because of regions having different refractive indices. The ray is split by a prism (called a Wollaston prism) and after passing through a polarizing filter it is recombined using a second prism at the image plane. By using a rotating stage the image contrast can be varied. Using this technique it is possible to create very

attractive images, because of the enhanced contrast. Nomarski microscopes are more expensive than conventional VLMs because of the cost of the Wollaston prisms.

NSOM (near-field scanning optical microscopy, also known as SNOM). This is a broad and growing topic.

The idea is that the resolution in VLM is limited by λ . If the light source is a fiber with an aperture in the end and we detect the reflected/scattered light with the same fiber, then the spatial resolution is determined by the diameter of the fiber. The limitation is that since the aperture diameter is smaller than λ (Figure 10.2), the emerging wave is evanescent so the signal strength is small. The use of a laser provides the necessary intensity and defines λ . The usefulness of the technique relies on the ceramics sample having suitable features to scatter the light. The technique can be used for other wavelengths and other signals (e.g., Raman). The latter technique is still being developed.

IR and UV. Because semiconductors are transparent to IR radiation, defects in these materials can be examined with IR microscopy. A detector sensitive to IR is required. With IR and ultraviolet (UV) light, a con-

NSOM PARAMETERS
Aperture size: 25–10 nm
Tip/sample gap 5–50 nm

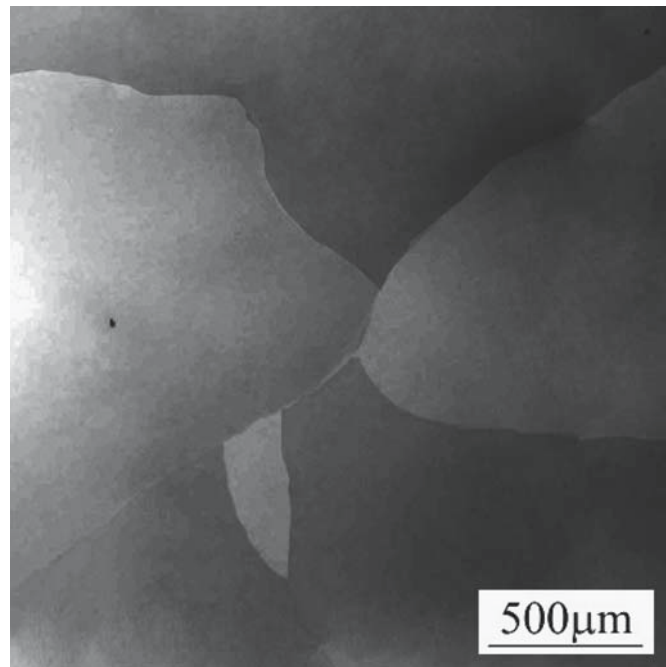


FIGURE 10.1 Slightly misoriented grains in a laser element imaged using polarized VLM. The crystal is yttrium orthovanadate with 0.27% Nd.

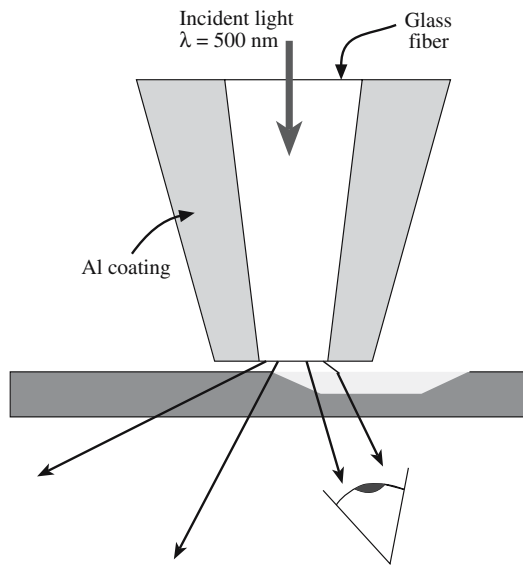


FIGURE 10.2 Schematic of the end of the fiber and the sample in NSOM.

verter or detector is also required. An advantage of UV microscopy is that because the wavelength of UV light is smaller than visible light the resolution of these microscopes is higher than VLMs. UV microscopy is widely used in the biological sciences to study sub-cellular structures. Using intense vacuum UV sources (available at national laboratories) it is possible to obtain results on, for example, electronic states.

10.3 IMAGING USING X-RAYS AND CT SCANS

X-ray topography can be used to obtain images of individual lattice defects in single crystals. This technique has been widely used to study crystal growth and, in particular, silicon. It can be used in

- Reflection (Berg–Barrett method)
- Transmission (Lang method or Borrmann method)

In either method it is the variation in intensity within the diffraction spot that is recorded. It is not usually the defects themselves that are imaged but rather the strain fields around them. These strains cause variations in plane spacing from their equilibrium value, thereby modifying the X-ray scattering process. Figure 10.3 shows a Lang topographic image of dislocations in potassium dihydrogen phosphate (KDP; KH_2PO_4). KDP has a relatively large electrooptic effect and can be grown as large strain-free crystals. X-ray topography has several advantages for characterizing defects in single crystals. It is nondestructive, does not require ultrathin samples (as is required in

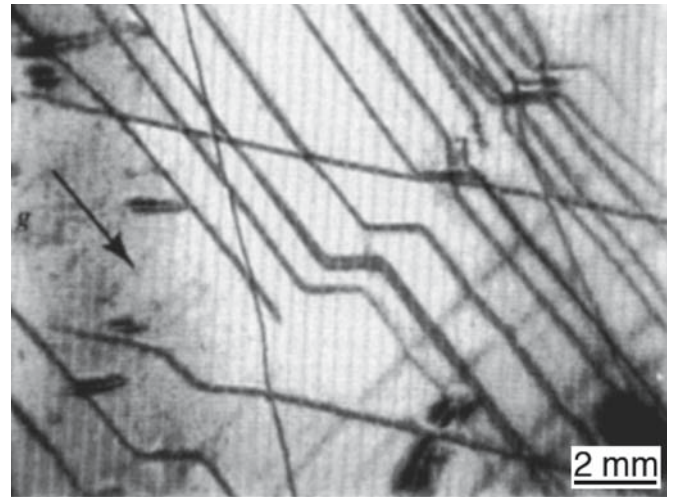


FIGURE 10.3 X-ray topography image showing dislocations in KDP imaged using a 022 reflection.

TEM), and can be used to observe very low dislocation densities (limit in TEM $>10^4 \text{mm}^{-2}$).

Computed tomography (CT) is used to determine inhomogeneities arising from local differences in density. It is applicable to a range of ceramics and minerals and is particularly useful for identifying defects in single crystals. The sample is placed on an automated stage that rotates as a series of X-ray images (radiographs) is captured (much like a medical CAT scan except that details as small as a few tens of micrometers can be resolved even in dense samples). A computer then processes the X-ray images and creates a three-dimensional (3D) reconstruction of the sample. Areas of lower density such as cracks and voids appear as darker contrast against a lighter background. Figure 10.4 shows density variations in the core of an Nd-doped YVO_4 sample.

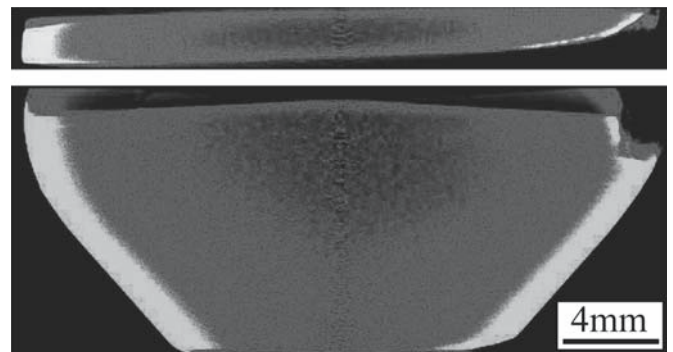


FIGURE 10.4 High-resolution X-ray CT images from the top and side of the same sample.

10.4 IMAGING IN THE SEM

The basic layout of the SEM is shown in Figure 10.5. The SEM can have two imaging detectors, one for secondary electrons (SEs) and one for higher-energy backscattered electrons (BSEs). The SEM typically has a resolution in SE mode of 0.7 nm (at 25 kV) and 2.5 nm in BSE mode at 5 kV. In addition to the excellent spatial resolution, the other great advantage of the SEM is that it has a much greater depth of field than the VLM (the depth of field is several millimeters). So the images appear more three-dimensional. The physical reason for this is that the electron beam is very narrow.

SEs are low-energy electrons so they are very sensitive to surface topology. Figure 10.6 shows an example of an SE image illustrating the excellent depth of field. BSEs are higher-energy electrons and are sensitive to the atomic number of the scattering atom. Hence the intensity of the BSE signal depends on a combination of the average atomic number and density of the ceramic. As the kilovolts are reduced, the scattering volume becomes more localized close to the surface of the sample. (The BSE electrons penetrate further into the sample and have further to come out after being scattered.) Hence the BSE image can give excellent mass discrimination even at low voltages. In

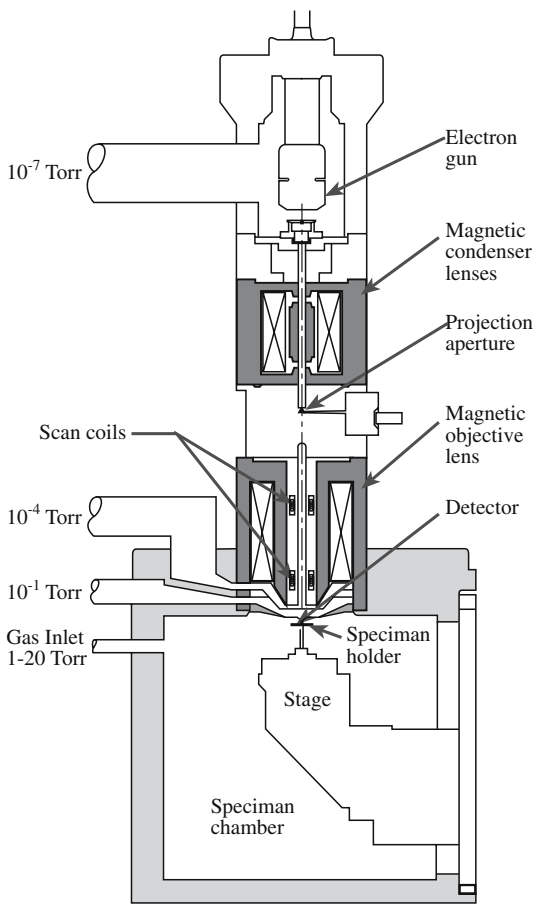


FIGURE 10.5 Schematic of an SEM showing examples of pressures used.

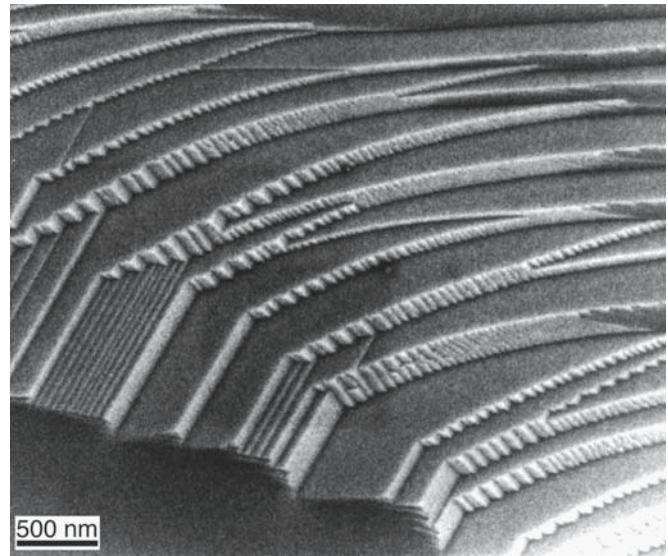


FIGURE 10.6 SE image showing steps on an alumina surface.

Figure 10.7 the three regions correspond to three different layers in a reaction couple. The MgO substrate is darkest, the In_2O_3 is lightest, and the spinel, MgIn_2O_4 , is intermediate. The very bright regions are Pt nanoparticles.

Charging in the SEM is usually avoided by coating the specimen (e.g., with a 1-nm layer of Pt). Working at lower accelerating voltages can also reduce charging effects, but then the resolution is compromised; electron lenses work better at higher resolutions. In low-voltage SEM imaging, you are trying to balance the electrons emitted as the specimen is irradiated with the charge building up on the specimen. Another way to avoid applying a conductive coating is to use an environmental or low-vacuum SEM. Then, the charging of the specimen is essentially grounded by the gas in the chamber. Variations in the SEM are summarized in Table 10.2.

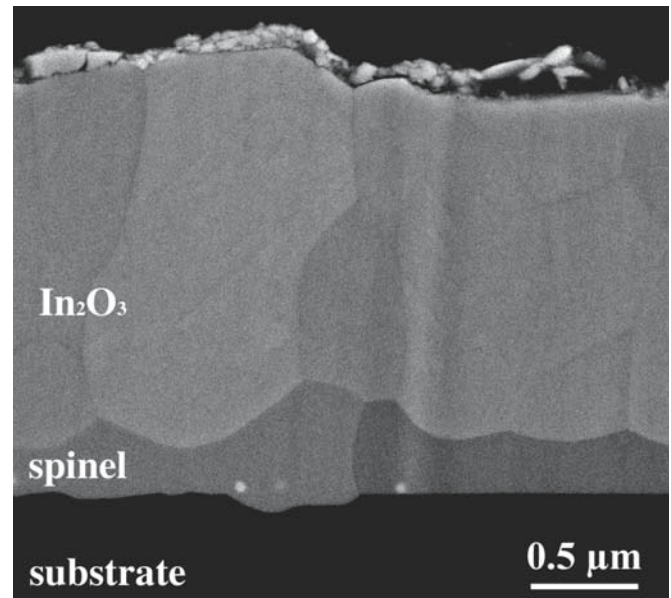


FIGURE 10.7 BSE image showing different contrast from different materials in an $\text{MgO}/\text{In}_2\text{O}_3$ reaction couple.

Signal	Energy	Source	Use
Secondary electrons	~5 eV	Loosely bound electrons scattered from surface	Main signal for image formation
Backscattered electrons	Energies up to incident beam energy	Beam electrons scattered back after collision	Atomic number contrast, channeling patterns, magnetic contrast
Characteristic X-rays	Discrete values for each element	Interband transitions usually involving K and L	Chemical analysis
Light (cathodoluminescence)	UV, visible, IR	Interband transitions between higher energy levels	Imaging dislocations in semiconductors

Environmental SEMs allow operation at pressures of several torr (0.1–20 torr) in the sample chamber and at temperatures >1000°C. In addition to being able to examine insulators it is also possible to follow dynamic processes such as drying of cement and crystallization.

10.5 IMAGING IN THE TEM

Figure 10.8 shows a state-of-the-art TEM with a field emission source. The key requirement for using TEM

RESOLUTION

The higher the resolution the smaller the features we can resolve.

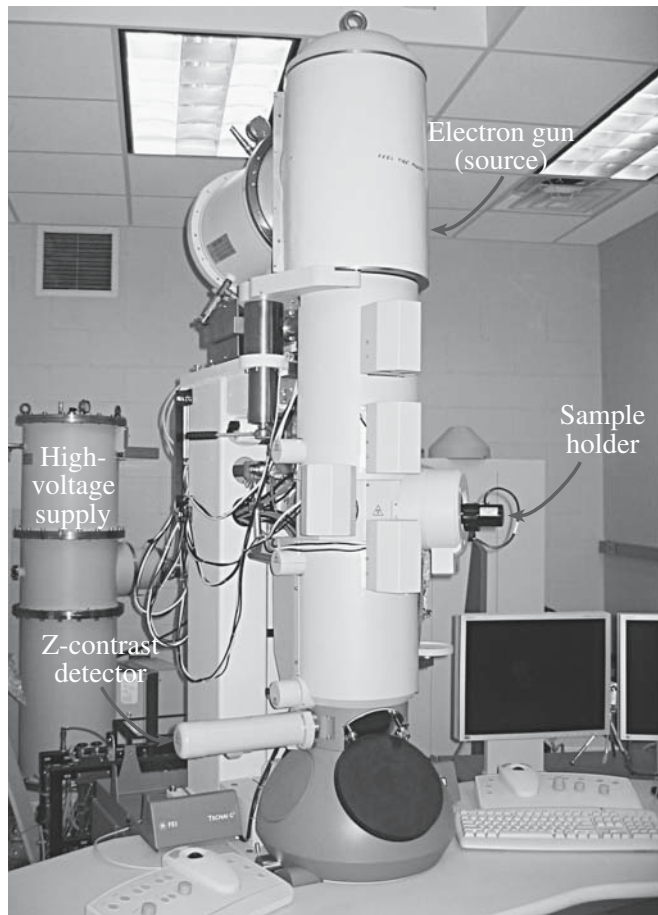


FIGURE 10.8 A TEM with key features labeled.

is that we require the sample to be very thin (usually ≤ 200 nm). So the technique is destructive and specimen preparation can be time consuming. The benefits, however, are significant. Because of the large range of signals generated by the incident electron beam (Figure 10.9), a TEM allows full characterization of a sample at high resolution. The conventional imaging modes in a TEM are bright-field (BF) imaging and dark-field (DF) imaging. In BF

imaging the image is formed using only the direct beam. An aperture (the objective aperture) is used to exclude all the diffracted electrons from contributing to the image. In DF imaging the image is formed from one of the elastically scattered beams and the objective aperture blocks the direct beam and all the other scattered electrons. The BF image in Figure 10.10a shows a thick particle of NiO sitting on a thin film of Al₂O₃; the different gray levels in the films correspond to different thicknesses in the Al₂O₃ film. The DF image in Figure 10.10b shows the same region after reacting the two oxides at high temperature; by using a reflection that is excited only by the spinel product, we can see exactly where the spinel has formed.

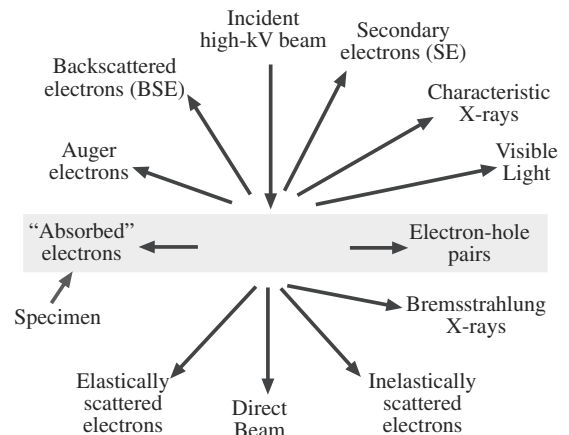


FIGURE 10.9 Signals produced in a TEM.

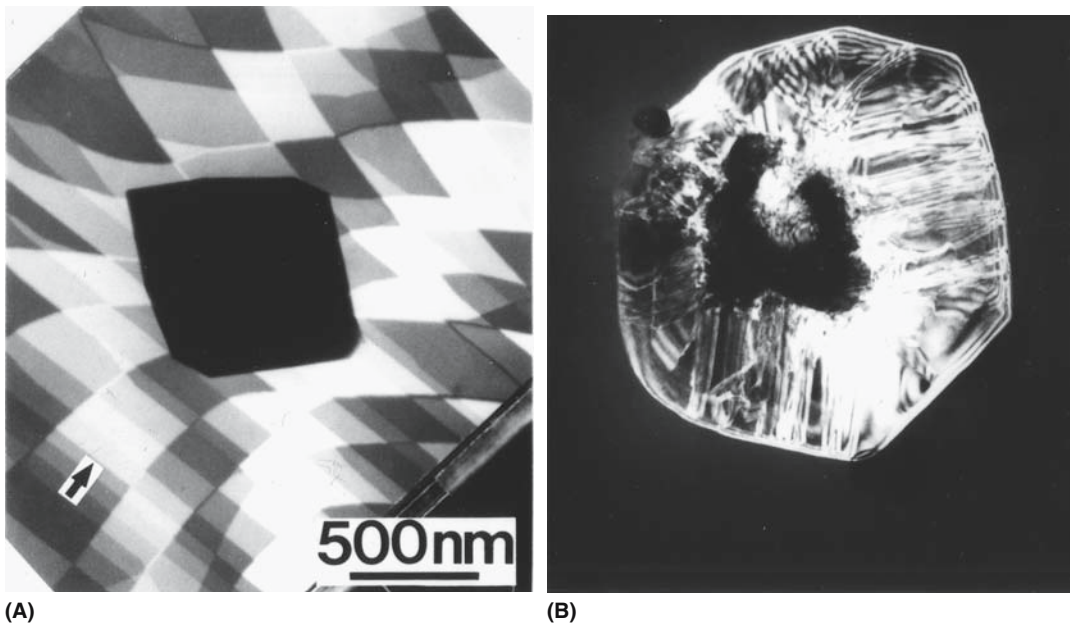


FIGURE 10.10 (a) BF and (b) DF image (using a spinel reflection) of a particle of NiO on a film of Al₂O₃ before and after reaction.

The resolution of a TEM is determined by the energy of the electrons (controlled by the accelerating voltage), the thickness of the specimen (we want to avoid multiple scattering within the sample), the distance between the sample and the objective lens, and the inherent quality of the lens (defined by its spherical aberration coefficient). Figure 10.11 shows an image of SrTiO₃ showing variations in the oxygen occupancy. At present, the best high-resolution TEM (HRTEM) has a resolution of ~0.08 nm (sub-Å!), but 0.05 nm should be achievable. For nanotechnology an HRTEM is an essential tool. An example is its use in studying crystals of KCl grown in a carbon nanotube as shown in Figure 10.12.

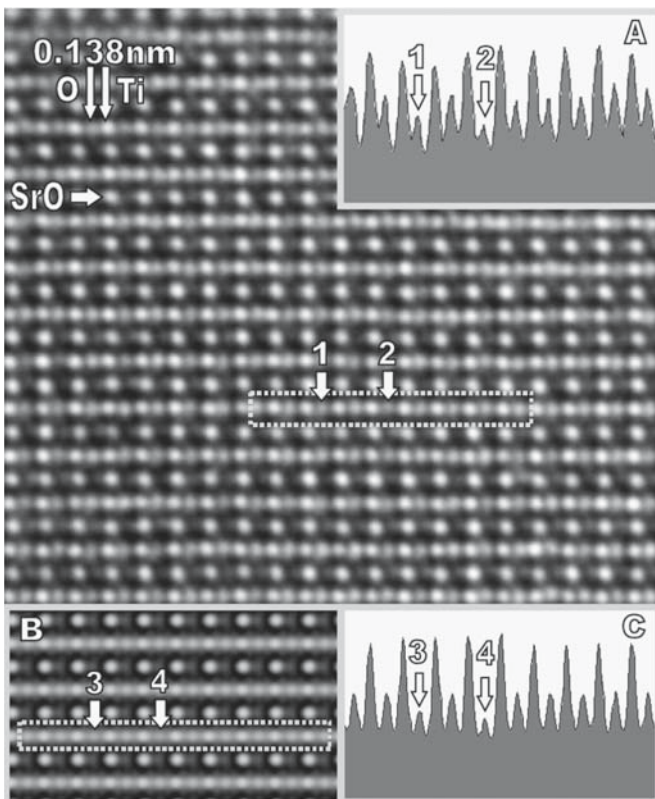


FIGURE 10.11 HRTEM image of the structure of SrTiO₃.

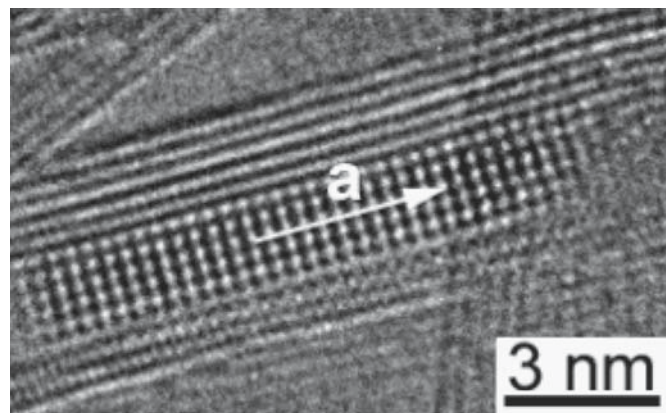


FIGURE 10.12 HRTEM image of a C nanotube partly loaded with a crystal of KCl.

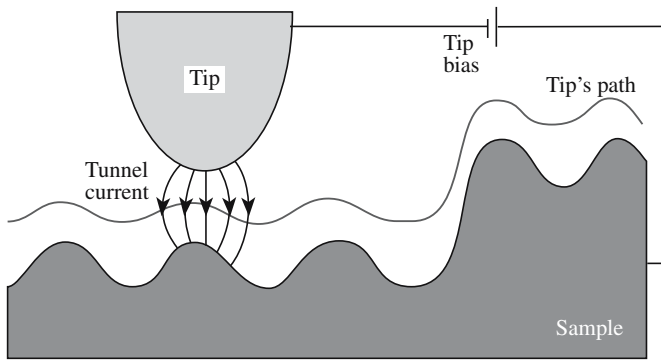


FIGURE 10.13 Schematic of the tip/sample interaction in STM; the tip does not make physical contact with the sample.

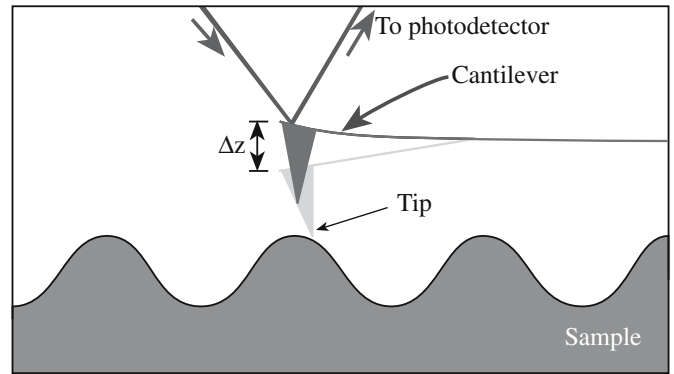


FIGURE 10.15 Schematic of the tip/sample interaction in AFM using a cantilever system.

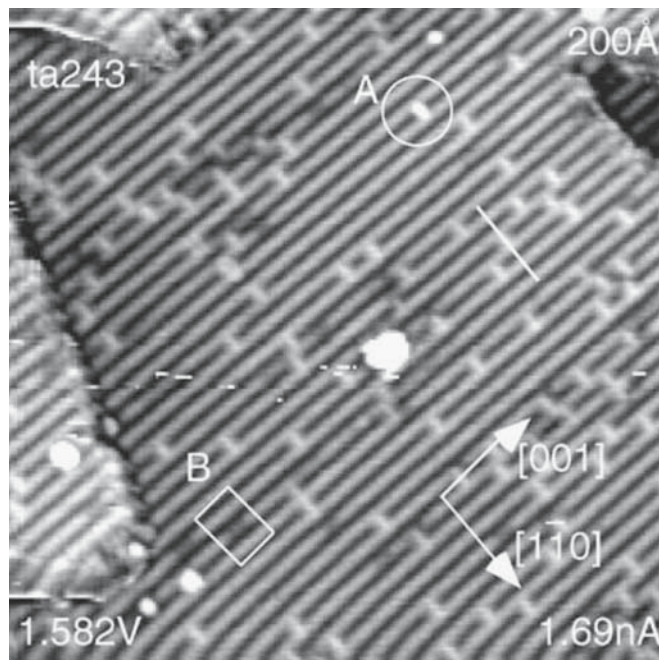
10.6 SCANNING-PROBE MICROSCOPY

The topic of scanned probe microscopy includes several different techniques, which grew out of the development of scanning tunneling microscopy (STM) (for which Binnig and Rohrer shared the Nobel Prize in 1986). The basic principle is that the tip of the probe determines the resolution of the image as shown in Figure 10.13. Scanning tunneling microscopy has been used to study the atomic structure of ceramic surfaces. Figure 10.14 shows the reconstructed (110) surface of TiO_2 . In addition to STM there are now several other types of scanned

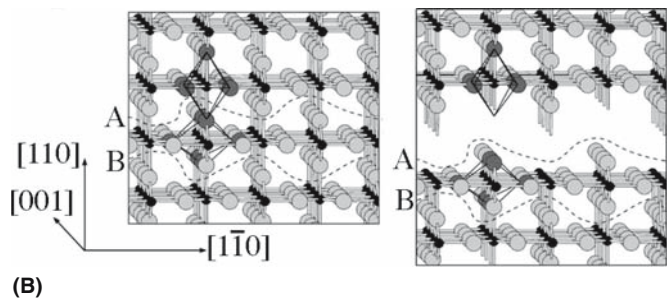
AFM AND STM “IMAGE” ATOMS

Both AFM and STM provide atomic resolution, meaning we can resolve individual atoms.

probe microscopy. The most widely used is atomic-force microscopy (AFM), which is illustrated in Figure 10.15. Atomic-force microscopy is extensively used to study the surfaces of nonconducting oxides. A pair of AFM images at low and high magnification is shown in Figure 10.16. The lines are straight single steps (0.4 nm high) on the surface of (111) spinel; the high-magnification image shows the origin of the steps as a pair of dislocations emerging at the surface. A nanoscale indenter can be attached to the AFM making it into an indenter with integrated imaging. Table 10.3 summarizes the common operating modes of the AFM.



(A)



(B)

FIGURE 10.14 STM image of the (110) surface of TiO_2 . The features labeled 'A' have been assigned as oxygen vacancies; the features labeled 'B' have not been identified. The schematics show the TiO_2 structure (compare to Fig. 6.11) and a model showing the proposed surface reconstructon.

10.7 SCATTERING AND DIFFRACTION TECHNIQUES

The fundamental idea is that we scatter particles or waves from the constituent atoms in the sample. If the waves interfere constructively, we have diffraction, which implies that the sample is at least partly crystalline. If the sample is not crystalline, we may still learn about the distribution of the atoms from the radial distribution function (rdf). The process of scattering generally implies particles; diffraction generally suggests Bragg diffraction or constructive interference of waves.

We can summarize some techniques in diffraction and scattering (of photons, electrons, neutrons, etc.).

Photon scattering	Raman and Fourier transform infrared (FTIR) are well-known techniques for the chemist and are increasingly important in ceramics
Electron diffraction	Selected-area diffraction (SAD) in the TEM Convergent-beam electron diffraction (CBED) in the TEM Electron-beam backscattering diffraction (EBSD) in the SEM Reflection high-energy electron diffraction (RHEED) in UHV for surfaces
Ion scattering	Rutherford backscattering spectrometry (RBS)
X-ray diffraction	Powder diffraction for statistical determination of lattice spacings Laue back-reflection for orienting single crystals
Neutron scattering	Small-angle scattering in a range of environments

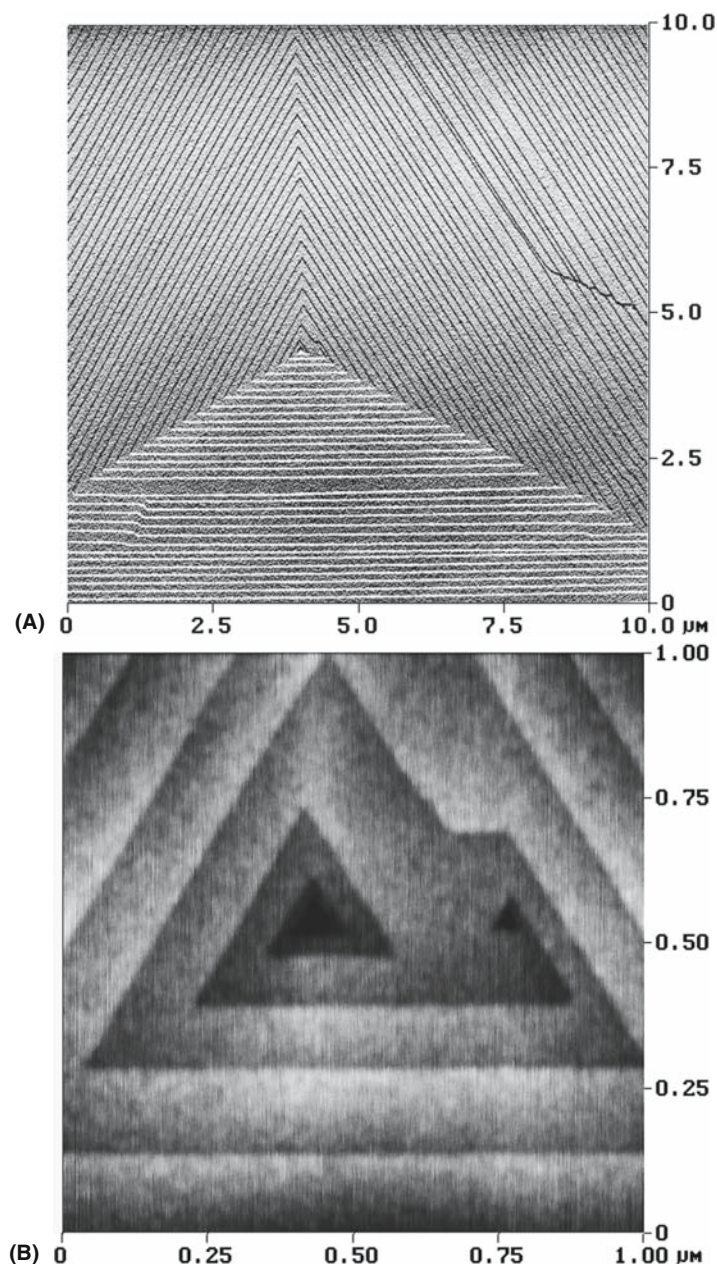


FIGURE 10.16 AFM image showing long (up to $10\mu\text{m}$) straight steps on the surface of an Mg–Al spinel. The steps are 0.4nm high. The lower image shows the central region at higher magnification.

TABLE 10.3 Modes of Operating the Atomic-Force Microscope

Mode of operation	Force of interaction
Contact mode	Strong (repulsive); constant force or constant distance
Noncontact mode	Weak (attractive)-vibrating probe
Intermittent contact mode	Strong (repulsive)-vibrating probe
Lateral force mode	Frictional forces exert a torque on the scanning cantilever
Magnetic force	Magnetic field of the surface is imaged
Thermal scanning	Variation in thermal conductivity is imaged

Electrons interact most strongly with the sample, so for transmission the specimen must be thin and in a vacuum. Neutrons are at the other extreme, but can be used only in dedicated (usually national) facilities because they require radioactive sources.

We will use diffraction in the TEM to study the crystallography of the interfaces and characterize other crystal defects. Bragg made the first direct determination of a crystal structure using X-ray diffraction (XRD), which is still generally the most accurate method for characterizing crystal symmetry, providing the sample is large enough and can be isolated. However, XRD does not provide a high spatial resolution because the beam diameter is typically 1mm , although with a rotating anode generator it may be 0.1mm and with a synchrotron $1\mu\text{m}$ or less is possible.

TABLE 10.4 Electromagnetic Spectroscopy

E (eV)	10^{-7}	10^{-5}	10^{-2}	10^{-1}	10^1	10^3	$>10^3$
T (K)	1.16×10^{-3}	1.16×10^{-1}	1.16×10^2	1.16×10^3	1.16×10^5	1.16×10^7	$>10^7$
ν (Hz)	2.4×10^{-7}	2.4×10^9	2.4×10^{12}	2.4×10^{13}	2.4×10^{15}	2.4×10^{17}	$>10^{17}$
λ (cm)	1.24×10^3	1.24×10^1	1.24×10^{-2}	1.24×10^{-3}	1.24×10^{-5}	1.24×10^{-7}	$>10^{-7}$
Radiation	Radio	Micro	IR	VIS	UV	X	γ
Atomic subsystem transitions	Nuclear spins	Electron spins	Rotation vibration	Outer shell electrons	Inner shell electrons		Nuclei
Primary quantity measured	Local interactions (magnetic, electric field gradient)		Atomic molecular potentials	Energy levels		Energy levels	Energy levels
Kinetic parameter detected	Diffusional atomic motions		Vibrational frequencies	Macroscopic, real time kinetic coefficients, point defect concentrations			
Effects on reactivity			Transport activation by heat	Photochemistry		Radiation chemistry	
Characteristic sample dimension (cm)	10^{-1} – 10^0	10^{-2} – 10^{-1}	ca. 10^0	10^{-4} – 10^0		10^{-2} (A1, 10^4 eV)	10^{-3} [Fe(MS)] 10^{-1} [In(PAC)]
Examples of methods	NMR	ESR	Raman	Absorption spectroscopy		XAS	Mössbauer, PAC

10.8 PHOTON SCATTERING

Electromagnetic spectroscopy involves the interaction of electromagnetic waves and matter. We can use all regions of the electromagnetic spectrum and each will give specific information about a material. Table 10.4 provides a summary and succeeding sections deal with each of the methods in a little more detail with specific application to ceramics. Once again, to really understand each of the methods you need to read a specialist text.

10.9 RAMAN AND IR SPECTROSCOPY

Raman and IR spectroscopy both involve the scattering of light. In IR spectroscopy, the light is polychromatic and couples to vibrational modes in the solid through dipole moments, which are associated with the vibration. These vibrational modes cause a dip in the transmission spectra or a peak in the absorption spectra. The IR range is from 0.78 to 1000 μm ($12,820$ to 10 cm^{-1}). The region where most fundamental vibrational modes occur, which is the most useful for materials characterization, is between 2.5 and 25 μm (4000 – 400 cm^{-1}). This is sometimes called the mid-IR region. The light source is a heated ceramic (usually a conducting ceramic or a wire heater coated with ceramic) that emits a range of frequencies.

- Spectroscopy: the art of using a spectroscope
- Spectrometry: the act of using a spectroscope

An important variant is the FTIR spectrometer. The main advantages of FTIR are that it is much quicker because it measures all the frequencies simultaneously and it is more sensitive than dispersive IR spectrometers.

Cryo-cooled HgCdTe detectors are used for weak signals or high resolution. The key component of an FTIR is the interferometer, which can be understood by considering the Michelson interferometer shown in Figure 10.17. A parallel beam directed from the source is split at B_s so that 50% of the light is transmitted and reflected back by mirror M_f , while the rest is reflected at B_s and then again at M_m . The beams recombine at B_s . The recombined beam will show constructive or destructive interference depending on the difference in the path lengths B_s to M_f and B_s to M_m . As M_m is moved smoothly toward or away from B_s the detector sees a signal that alters in intensity. If the recombined beam from B_s is passed through a sample before reaching the detector sample absorptions will show up as gaps in the frequency distribution. The complex intensity distribution received by the detector is Fourier transformed by a computer to produce an absorption spectrum.

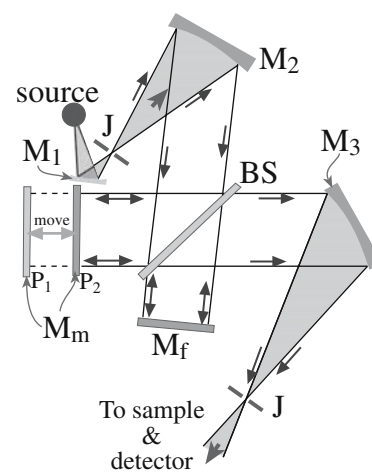


FIGURE 10.17 Schematic of the arrangement of mirrors and ray paths in FTIR.

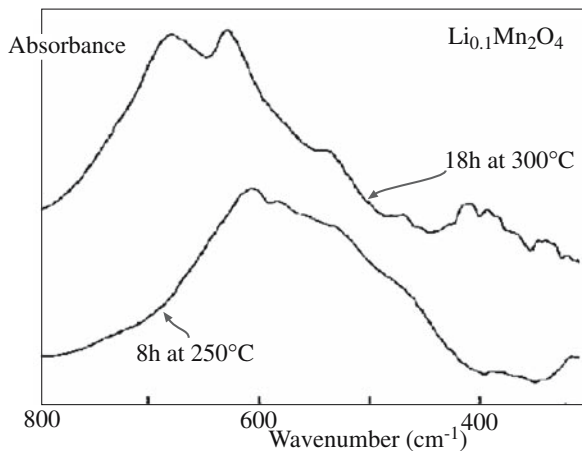


FIGURE 10.18 FTIR absorption spectra from $\text{Li}_x\text{Mn}_2\text{O}_4$ insertion electrodes after different heat treatments.

IR spectra are output in the form of plots of intensity (percent transmittance, % T , or absorbance, A) versus either energy (in J), frequency (in Hz), wavelength (in μm), or wavenumber (in cm^{-1}). The use of wavenumber is preferred, but some of the standard reference sources of IR spectra use wavelength. FTIR can be used to determine the oxygen content in silicon. The Si–O stretching band occurs at 1105 cm^{-1} and from the peak intensity the oxygen concentration can be determined using ASTM standard F 121. The FTIR absorption spectra in Figure 10.18 is from $\text{Li}_{0.1}\text{Mn}_2\text{O}_4$ after heating for 8 hours at 250°C and 18 hours at 300°C . These FTIR readily distinguishes them from the binary oxide MnO_2 .

In Raman spectroscopy, the light is nearly monochromatic and is usually in the visible range. The light source is a laser, e.g., a 50-mW 785-nm diode laser. Raman spectroscopy has become a routine tool for exploring the structure and chemical properties of materials. It can provide more information than IR spectroscopy. There are three types of signal in a typical Raman experiment as illustrated in Figure 10.19.

The scattering process can be anti-Stokes, Rayleigh, or Stokes. We are then interested in measuring the intensity and the Raman shift.

In *Rayleigh scattering*, a molecule is excited by the incident photon to a virtual energy level. This energy level is caused by a distortion of the electron distribution of a covalent bond. The molecule returns to the vibrational ground state by emitting the same energy, E_0 ($E_0 = h\nu_0$). Rayleigh scattering is an elastic process.

Vibrational excitations can be created, which causes a decrease in the frequency (i.e., in energy) of the scattered light, or they can be annihilated, which causes an increase. The decrease in frequency is called *Stokes scattering* and the increase is *anti-Stokes scattering*. Stokes scattering is the normal Raman effect and Raman spectroscopy generally uses Stokes radiation.

Figure 10.20 shows a typical Raman spectrum. It is a plot of scattered light intensity as a function of frequency

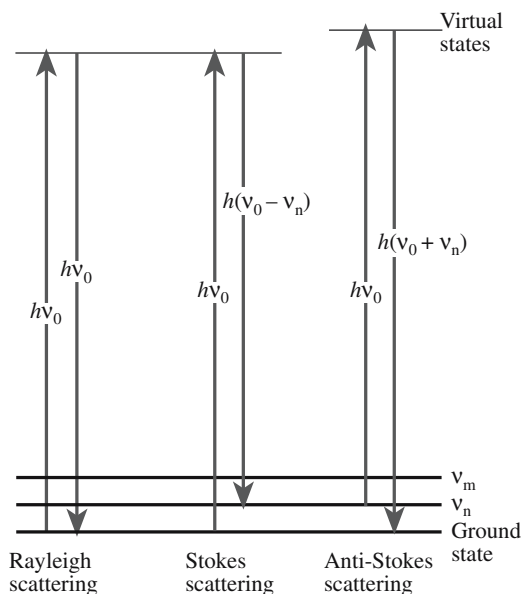


FIGURE 10.19 Schematic of transitions occurring in Raman spectroscopy.

shift (Raman shift in cm^{-1}) in which the shift is calculated relative to the laser line frequency that is assigned as zero. The material is TiO_2 films prepared by the sol-gel technique that have been annealed at temperatures between 400°C and 800°C . The features in the spectra correspond only to anatase until the film reaches 800°C . At this temperature, a mixed anatase–rutile phase is seen, while the pure rutile phase is obtained only at 900°C .

There are increasing applications for Raman spectroscopy. One application is its use in the identification of different pigments in the characterization of historical artifacts. Table 10.5 lists blue pigments used on or before about 1850 that have been identified by Raman spectroscopy.

Variations in Raman spectroscopy include the following:

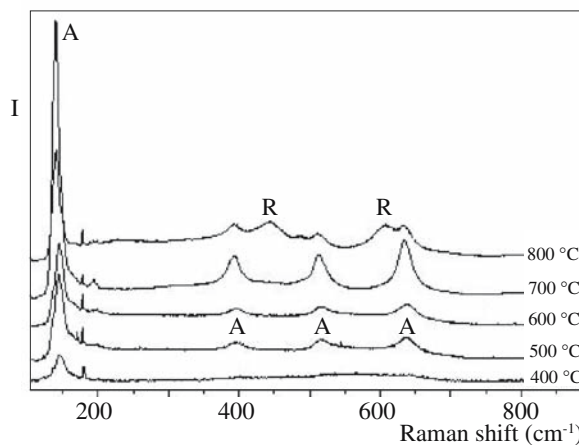


FIGURE 10.20 Example of Raman spectra from TiO_2 films heated to different temperatures. R, rutile; A, anatase.

TABLE 10.5 Blue Pigments Identified by Raman Spectroscopy

Name	Composition	Band wavenumbers, cm^{-1} and relative intensities	Excitation λ and power	Notes and date
Azurite	Basic copper(II) Carbonate $2\text{CuCO}_3 \cdot \text{Cu}(\text{OH})_2$	145w; 180w; 250m; 284w; 335w; 403vs; 545w; 746w(sh); 767m; 839m; 940w; 1098m; 1432m; 1459w; 1580m; 1623vw	514.5 nm 2 mW	Mineral
Cerulean blue	Cobalt(II) stannate $\text{CoO} \cdot n\text{SnO}_2$	495m(sh); 532s; 674vs	514.5 nm 4 mW	1821
Cobalt blue	Cobalt(II)-doped alumina Glass, $\text{CoO} \cdot \text{Al}_2\text{O}_3$	203vs; 512vs	514.5 nm 4 mW	1775
Egyptian blue	Calcium copper(II) Silicate, $\text{CaCuSi}_4\text{O}_{10}$	114m; 137m; 200w; 230w; 358m; 377m; 430vs; 475m(sh); 571w; 597vw; 762w; 789w; 992w; 1012w; 1040w; 1086s	514.5 nm 4 mW	3000 BC; also known as cuprorivaite
Lazurite	S3- and S2- in a sodium aluminosilicate matrix $\text{Na}_8[\text{Al}_6\text{Si}_6\text{O}_{24}]\text{Sn}$	258w; 548vs; 822w; 1096m	514.5 nm 4 mW	Mineral (lapis lazuli) Synthetic c.1828 = ultramarine
Posnjakite	Basic copper(II) sulfate $\text{CuSO}_4 \cdot 3\text{Cu}(\text{OH})_2 \cdot \text{H}_2\text{O}$	135vw; 208vw; 278vw; 327vw; 467w; 612w; 983vs; 1092vw; 1139vw	632.8 nm 3 mW	Mineral
Prussian blue	Iron(III) hexacyanoferrate(II) $\text{Fe}_4[\text{Fe}(\text{CN})_6]_3 \cdot 14\text{-}16\text{H}_2\text{O}$	282vw; 538vw; 2102m; 2154vs	514.5 nm 2 mW	1704; earliest synthetic modern
Smalt	Cobalt(II) silicate $\text{CoO} \cdot n\text{SiO}_2$	462vs; 917m	514.5 nm 2 mW	~1500

Laser Raman Microprobe: This allows information to be collected from small samples via the use of a VLM, which allows the region to be selected from which the Raman spectrum will be obtained. Surface-Enhanced Raman Scattering (SERS): This is used to examine surfaces, oxidation, catalysis, and thin films.

Residual Stress Measurement: Scattering depends on local stress, which can be probed in regions as small as $0.7 \mu\text{m}$ in diameter by Raman spectroscopy.

Fortunately, there are many isotopes, such as ^{29}Si , ^{27}Al , and ^{11}B , that are important for ceramics that are suitable. Notice that we have to use ^{29}Si ($I = 1/2$) not the more abundant ^{28}Si .

When a nucleus that has a nonzero P_I is subjected to a magnetic field of strength H , the energy levels are split into $2I + 1$ different values. The energy separation of the different levels is

$$\Delta E = \gamma H h / 2\pi \tag{10.2}$$

10.10 NMR SPECTROSCOPY AND SPECTROMETRY

Just as each electron has a spin of $\pm 1/2$, each neutron and proton in the nucleus also has a spin, I , of $1/2$. These spins combine so that each atom has a total nuclear spin of 0, $1/2$, or 1, and an angular momentum P_I , given by

$$P_I = (h/2\pi)\sqrt{I(I+1)} \tag{10.1}$$

The principle of nuclear magnetic resonance (NMR) is that the probing beam is tuned until it couples with the natural angular momentum of the nucleus, which then resonates and emits energy that is measured. The specific quantities depend on the atom that is resonating. The precise value of the energy involved changes slightly if the electron distribution around the resonating nucleus changes, as is the case when the atom is bonded to other atoms; we use NMR to examine this chemical shift. Nuclear magnetic resonance thus probes the bonding of individual atoms. Clearly for the technique to be applicable, the nucleus must have a nonzero total nuclear spin.

γ is called the gyromagnetic ratio of the nucleus. If we then subject this nucleus to electromagnetic radiation and adjust the frequency, ν , to be ν_0 , so that it has the same energy ΔE (now $h\nu_0$), the quanta of radiation can be absorbed as transitions between the different nuclear spin energy levels occur. We then detect the NMR absorption in the spectrum as a single peak corresponding to ν_0 , which is broadened because the atoms interact differently depending on their neighbors.

There are two particularly important interactions to consider:

- The dipole interaction is the interaction between adjacent nuclei and the one you are probing (such as an interaction between magnetic dipoles).
- The electrons surrounding the nucleus will also move because of the applied magnetic field; this is the chemical shift—electrons determine chemistry.

The technique can be carried out using either a continuous wave (CW) or a pulsed spectrometer. The RF energy is used to excite the nuclear magnetization. The measurement is the response of the spin system to this excitation. In CW the nuclear magnetization is irradiated at a

constant level; the frequency of the irradiation or the magnetic field is then swept across the resonance.

Nuclear magnetic resonance systems are available in most research universities with a basic system costing from \$200,000 up to more than \$1,000,000, depending mostly on the desired field strength (1–14 T).

The following examples are selected to illustrate why NMR is so valuable for the ceramist. The x -axis is in units of ppm, which is the chemical shift as a fraction of the applied field or frequency. In Figure 10.21, three NMR powder patterns are shown for silicon in three different chemical environments, but where the Si is tetrahedrally coordinated in each case. The differences between the spectra are due to the number of nonbridging oxygen ions that are attached to the Si nucleus being probed: a chemical-shift effect. The value of NMR for studies of silicate glass is obvious.

Figure 10.22 shows a series of NMR spectra from Si–Al glasses. The field used was 11.7 T. The NMR spectra show that not only is the Al present in 4-fold, 5-fold, and 6-fold coordination, but there is also undissolved Al_2O_3 present in the glass (denoted “Cor” in the spectra). The chemical shift has been determined using a standard of octahedral ^{27}Al in AlCl_3 solution.

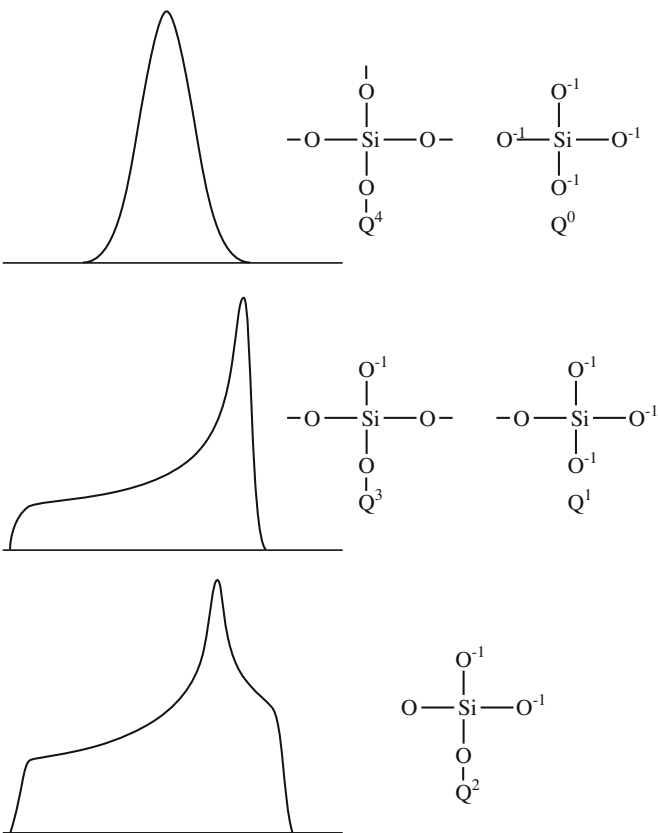


FIGURE 10.21 NMR signals from Si.

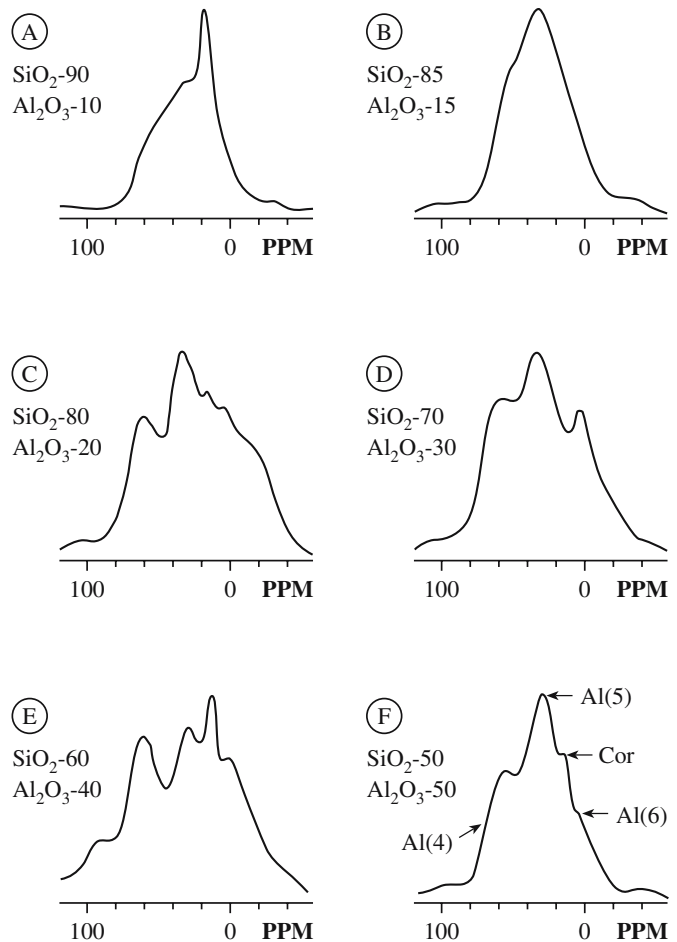


FIGURE 10.22 NMR signals from an Al–Si glass.

10.11 MÖSSBAUER SPECTROSCOPY AND SPECTROMETRY

Mössbauer spectroscopy is specialized, but it can be invaluable when it is available. The technique relies on the recoil-free emission and resonant absorption of γ -rays by nuclei that are bound in the solid state. (If it is not in a solid, the free nucleus recoils and no resonance is detected.) To see this resonance, we have to match the energy of the γ -ray emitter to the energy of the absorber (the sample), which means that only a small number of elements can be studied. Two that can be studied are tin and iron. The technique gives information on the bonding and coordination, and on the valence (oxidation) state. Since the technique relies on Z , it works for particular isotopes, ^{57}Fe for iron with ^{57}Co as the radioactive source of γ -rays. (Natural Fe contains ~ 2.19 wt% ^{57}Fe .)

Figure 10.23 shows a schematic of a Mössbauer spectrometer. The radioactive ^{57}Co source is embedded in a nonmagnetic matrix, which is chosen so as not to affect the sample or to absorb the γ -rays too strongly. The system can be calibrated using Fe metal; the six peaks seen in Figure 10.24 correspond to the six transitions expected for ^{57}Fe . The ^{57}Co source has an emission peak at 14.4 keV;

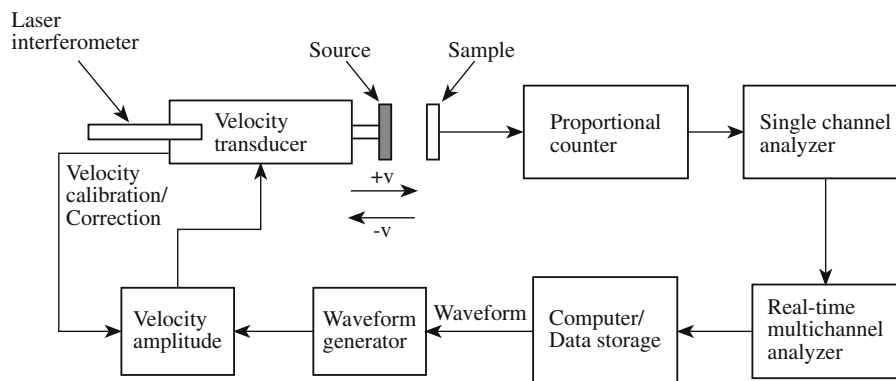


FIGURE 10.23 Schematic of the set-up for Mössbauer spectroscopy.

the source is moved through a range of velocities using a velocity transducer.

Mössbauer spectra from a series of glasses containing Fe in different oxidation states are shown in Figure 10.25. The differences in the curves are clear, but the analysis needed to determine the percentage of Fe in the 2+ state requires extensive calibration of the system. (Notice that peak locations are shown in units of velocity.) The value of the technique is its sensitivity to determining both the

oxidation state and the coordination of the Fe ion. Nuclei in different chemical surroundings from the source do not absorb at the same frequency; this is known as the chemical (or isomer) shift and is the key feature of Mössbauer spectroscopy.

Other isotopes that have been studied are ^{119}Sn (source: metastable ^{119}Sn), ^{121}Sb (source: metastable ^{121}Sb), and ^{151}Eu (source: ^{151}Sm). Table 10.6 lists chemical shifts for tin. It is then quite straightforward to determine the valence state of an unknown tin-compound from its Mössbauer spectrum. This type of analysis has been used in studying tin glazes and tin-containing ceramic pigments. It requires quite small amounts of material, typically 50 mg of powder. Bulk materials can also be examined.

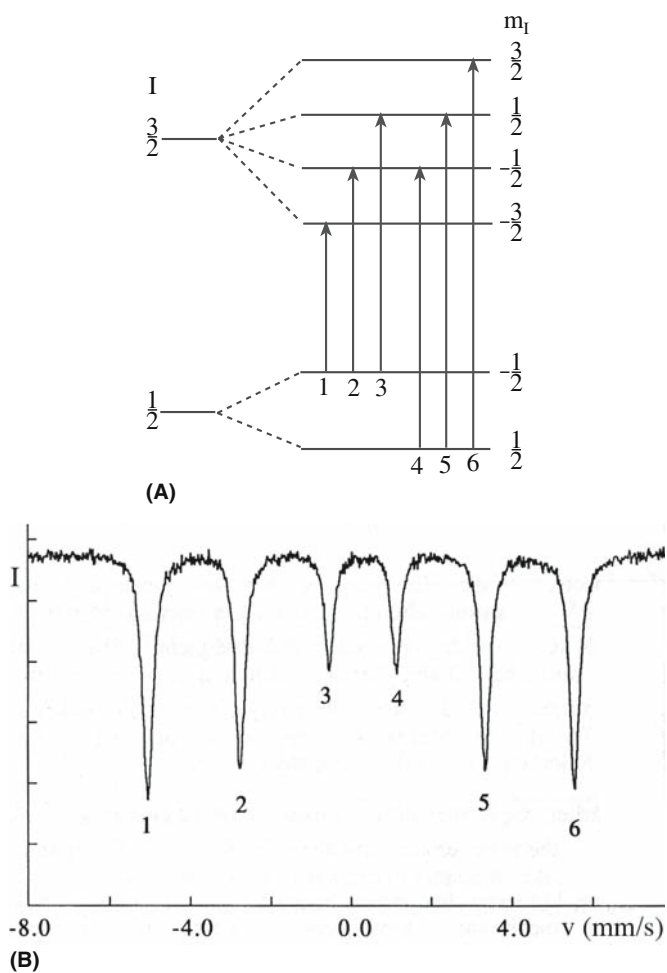


FIGURE 10.24 Transitions in Fe and the resulting Mössbauer spectrum.

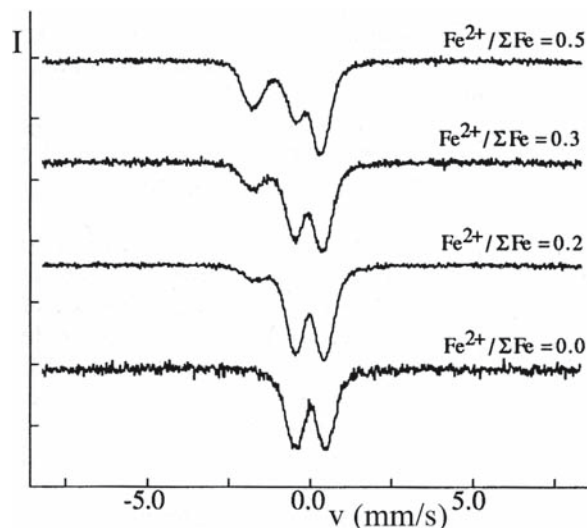


FIGURE 10.25 Mössbauer spectra from glasses containing different concentrations of Fe^{2+} .

TABLE 10.6 Chemical Shift of Some ^{119}Sn Compounds

Valence state	Electron configuration	Chemical shift (mm/s)
Sn^{4+}	$5s^05p^0$	0
Sn (4-covalent)	$5(sp^3)$	2.1
Sn^{2+}	$5s^25p^0$	3.7

10.12 DIFFRACTION IN THE EM

The techniques are

- SAD in the TEM
- CBED in the TEM
- EBSD in the SEM

Selected-area diffraction involves selecting an area on the sample (actually an image of the area) with an aperture and then looking at the diffracting pattern from that area. The diameter of the area can be as small as 100 nm with a modern machine. In CBED, the diffracting area is selected by focusing the electron beam onto a small area of the sample. The diameter of the area can actually be smaller than the unit cell. Figure 10.26 compares SAD and CBED patterns. From the positions of the spots (in SAD) and the discs (in CBED) we can obtain information about the structure and orientation of our sample. CBED patterns often contain an additional fine structure, which allows determination of symmetry such as the point group. The value of CBED lies in its ability to provide information on lattice parameters, sample thickness, and local crystallography on a scale of 10 nm or better. We can use the technique to characterize polarity change across antiphase boundaries (APBs) in GaN and AlN, to determine the site occupancy in nickel-titanate spinel, and to determine the thickness of a specimen. The latter parameter is used in analyzing the height of steps on surfaces and in quantifying X-ray energy dispersive spectrometry (XEDS) data.

Diffraction in the SEM can take several forms, but EBSD is now becoming a routine addition to the SEM. The beam penetrates into the sample and is backscattered; we can use these electrons to form a BSE image or we can record the actual diffraction pattern. A schematic of the

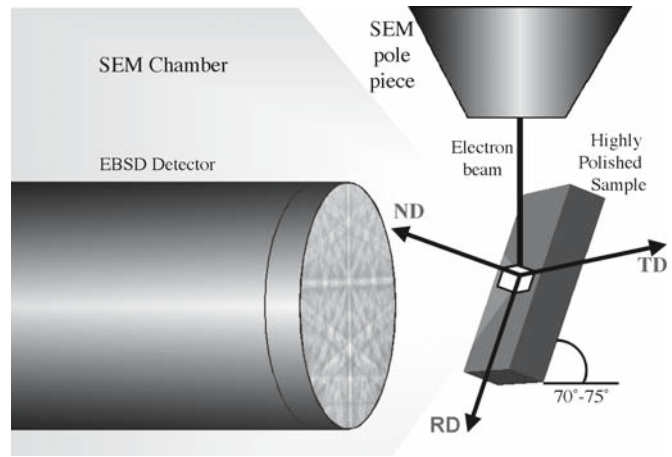


FIGURE 10.27 Schematic of the formation of an EBSD pattern.

system is shown in Figure 10.27 together with an example of an EBSD pattern.

10.13 ION SCATTERING (RBS)

Rutherford backscattering spectrometry again uses ions (a high-energy He beam) to produce the signal, but is more akin to electron energy loss spectroscopy (EELS). We analyze the energy of the backscattered ions and thus determine what atoms they interacted with and where those atoms were located in the sample relative to the surface. Rutherford backscattering spectrometry uses ions (typically 2 MeV helium ions, $^4\text{He}^+$) as the scattered particle. We can picture the interaction mechanism as being a collision resembling that between two billiard balls; the incoming ion transfers energy (and momentum) to the ion in the sample, it is detected as it recoils, and its energy is

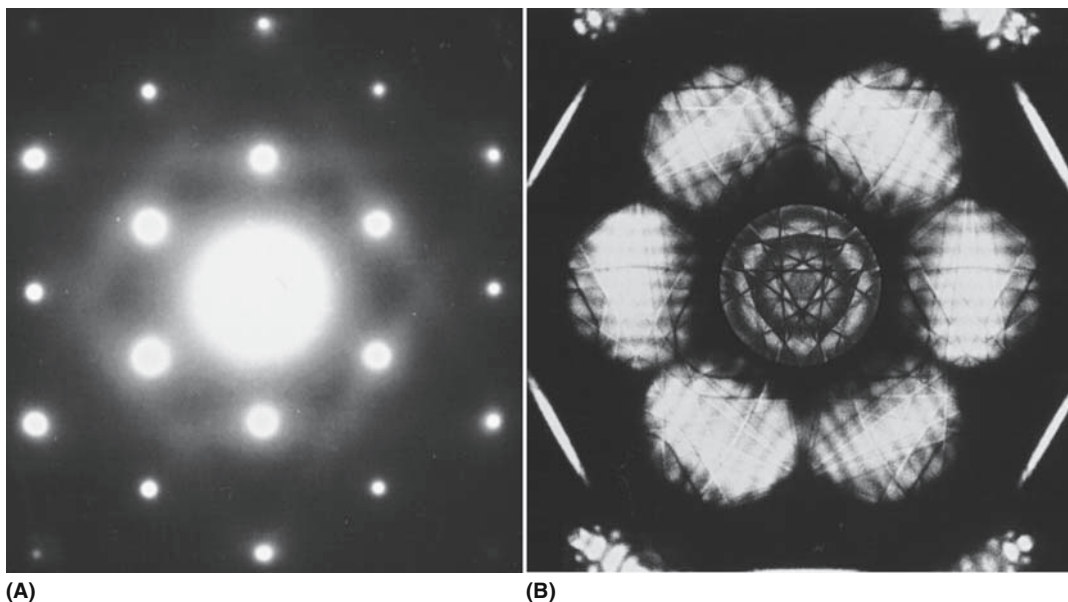


FIGURE 10.26 Diffraction patterns obtained using (a) SAD (TEM) and (b) CBED (TEM).

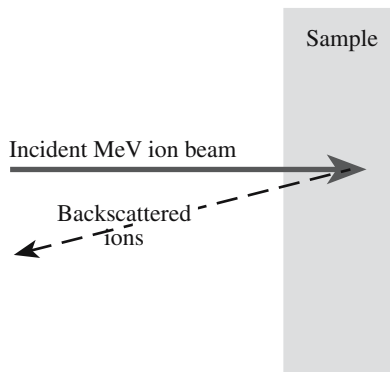


FIGURE 10.28 The backscattering process for RBS; the sample can be tilted to the beam to increase depth resolution.

determined (Figure 10.28). The data are provided in the form of a plot of backscattering yield versus energy and typical spectra are shown in Figure 10.29. Computer analysis of the spectrum gives us the types of atoms in a sample, their concentration, and their depth. The depth resolution is about 20 nm and RBS has been widely used in studies of ceramic thin films deposited onto ceramic substrates such as BaTiO₃ on MgO.

Rutherford backscattering spectrometry has a poor sensitivity to light elements such as oxygen and nitrogen, which are both important in many ceramics. However, an enhanced oxygen signal can be obtained at an incident energy of 3.045 MeV. It is also used to determine the composition of bulk ceramics and impurity profiles in semiconductors, e.g., As distribution in Si.

When the ion beam interacts with the sample, it produces particle-induced X-ray emission (PIXE), which is directly analogous to the production of X-rays in the SEM. Particle-induced X-ray emission has some special advantages over EDS in the SEM in that the background emission is lower, the depth penetration is large, and the sensitivity is high.

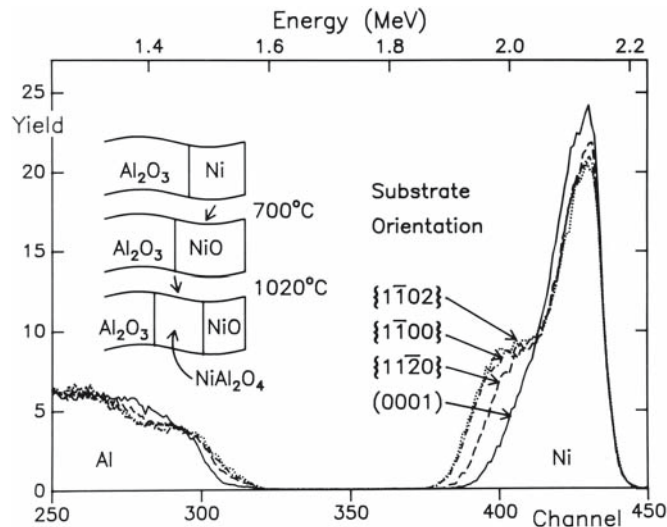


FIGURE 10.29 RBS data sets obtained using a 2.8-MeV beam of He²⁺ ions with the samples tilted 45°. Each sample has been annealed at 700°C for 2 hours followed by 1020°C for 5 hours; the Ni peak shows that the extent of the reaction varies with the surface orientation.

10.14 X-RAY DIFFRACTION AND DATABASES

X-ray diffraction is used in several forms depending on the equipment, the sample, and what you want to know. The great advantage of the technique is that a vacuum is not required and that the X-rays can travel through a container before and after interacting with the specimen. For example, the specimen can be heated inside a quartz tube to 1600°C and examined at that temperature. Using a synchrotron, the beam size and, hence, the spatial resolution can be reduced to ~1 μm. A monochromatic beam can be produced such that changes in energy due to absorption can be accurately measured. Table 10.7 lists types of analysis that can be undertaken using X-rays and the specific technique.

TABLE 10.7 X-Ray Diffraction Analysis		
Type of analysis	Method	Sample
Crystal geometry	Moving crystal-spot pattern	Single crystal
	Computer positioned diffractometer	Single crystal
	Solution of <i>d</i> -spacing equations	Powder
Arrangement of atoms	Analysis of diffracted intensities	Single crystal
	Refinement of whole pattern	Powder
Symmetry	Moving crystal-spot pattern	Single crystal
	Stationary crystal-spot pattern	Single crystal
Identification of compound	Identification of cell parameters	Single crystal
	Matching of <i>d</i> - <i>l</i> set	Powder
	Single-crystal back reflection	Large single crystal
Crystal orientation	Texture analysis	Powder compact
Size of crystal	Line broadening	Powder
Magnitude of strain	Line shifts	Powder compact
Amount of phase	Quantitative analysis	Powder
Change of state	Special atmosphere chambers	Single crystal or powder
Crystal perfection	Direct imaging	Single crystal
	Line shape analysis	Powder

One of the most useful sources of information for crystal structure data is the Powder Diffraction File (PDF). The PDF is a collection of single-phase X-ray powder diffraction patterns in the form of tables of interplanar spacings (d) and corresponding relative peak intensities. There are more than 80,000 patterns in the PDF. In the early days the patterns were printed as 3" × 5" index cards and even though everything is now on computer the files are still referred to as "cards."

Powder XRD is one of the most widely used techniques to characterize ceramics. The material is in the form of a powder so that the grains will be present in all possible orientations so that all d spacings, or θ values, will appear in one pattern. The classical powder pattern was recorded on photographic film. Now the data are in the form of a plot (known as a diffractogram) of counts or intensity versus scattering angle (2θ) as shown in Figure 10.30. A computer that contains the entire PDF is usually used for peak identification. In many examples you will see in the literature phase identification is the extent to which powder XRD is used. This ability alone makes it a powerful and indispensable tool for the ceramist. In a multiphase material the relative amounts of each phase can be determined from the peak areas.

Powder XRD can be used to estimate the sizes of particles. The Scherrer formula states that

$$\Delta\theta \cdot \Delta x = 2\pi \quad (10.3)$$

where $\Delta\theta$ is the peak width (scattering angle half-width) and Δx is the average particle diameter. The resolution of

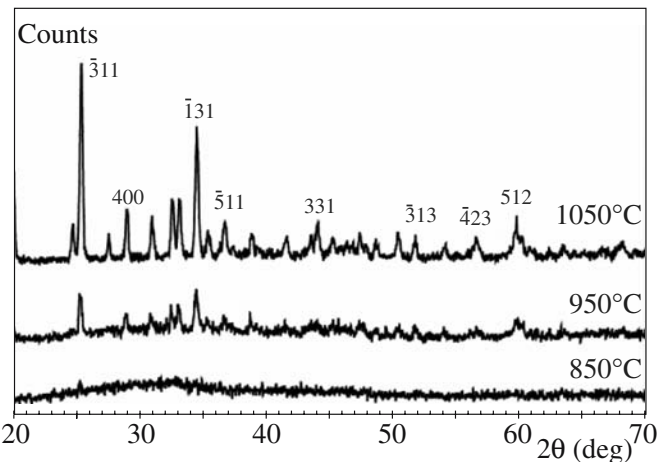


FIGURE 10.30 XRD patterns from a mixture of Ca oxide and alumina recorded while heating the sample at different temperatures.

PDF CARD NUMBERS

21–1272 Anatase
29–1360 Brookite

the diffractometer corresponds to an integral width of 0.32 nm.

Figure 10.31 shows the main components of an X-ray diffractometer. The important features include the following:

- X-ray source. Often Cu $K\alpha$ $\lambda = 0.154184$ nm because of its high intensity.
- Sample. Usually a powder, but it can be pressed or sintered. Only a few milligrams is needed.
- Detector. There are two main types: proportional detectors use photoelectrons generated in Xe; semiconductor detectors use electron-hole pairs created in p-i-n junctions formed in silicon.

In the $\theta/2\theta$ X-ray diffractometer, the sample and detector rotate relative to the X-ray source; when one moves through θ , the other moves through 2θ . Alternatively, the sample can be held fixed and the detector and source rotated in opposite directions. The conventional XRD geometry is often referred to as the Bragg–Brentano geometry. Several different geometries and modifications are used for studying ceramics.

Thin-film diffractometer. A glancing angle geometry is used with the sample surface at an angle of 5–10° to the X-ray beam. The basic idea is that the penetration depth of the X-rays is reduced so they are analyzing the surface. Longer wavelength X-rays can be used, which also reduces penetration (switch to a Cr $K\alpha$

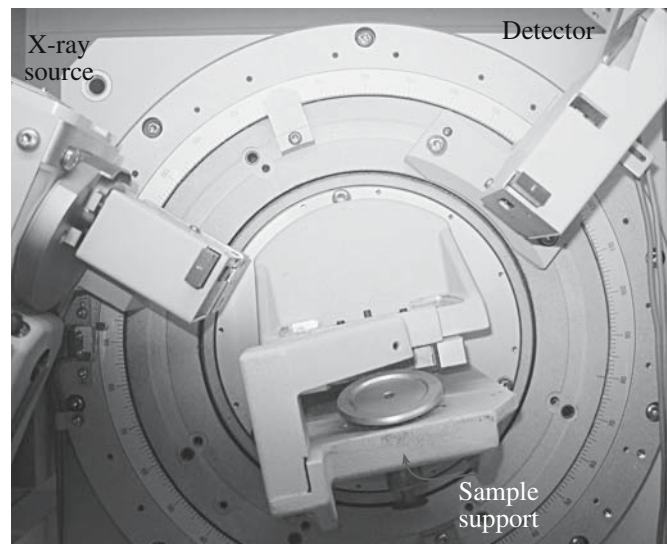


FIGURE 10.31 XRD apparatus showing the location of the source, sample, and detector (Siemens D5005).

source $\lambda = 0.229100\text{ nm}$). Polycrystalline thin films down to a few tens of nanometers thick can be examined.

Microdiffractometer. Collimators as small as $10\mu\text{m}$ are used to produce a small X-ray spot size. The geometry of the detection system is also different from a conventional diffractometer in that it uses an annular detector that allows sampling of the entire cone of diffracted radiation.

Hot-stage XRD. The sample is placed inside a quartz furnace tube that can be heated to temperatures up to 1600°C often in a range of different atmospheres. The main uses are to study phase changes and structural transformations as a function of temperature.

Pole figure. This uses a Eulerian goniometer cradle attached to the diffractometer to determine preferred crystal orientations.

Single-crystal XRD. A single-crystal diffractometer allows the orientation of the crystal to be controlled in such a way that every set of planes can be moved into a diffraction condition. The X-rays are usually detected by scintillation. The technique is not as routine as powder XRD and determination of a crystal structure can take many days or even turn into a thesis.

Laue technique. The diffracted beams produce a pattern consisting of an array of spots. It is used to orient single crystals (with an accuracy in a range of 0.3° to 1°) prior to cutting and polishing.

10.15 NEUTRON SCATTERING

The initial obvious statement is that, overall, neutrons interact with matter even less strongly than do X-rays. Table 10.8 summarizes the differences between the two probes. For both neutrons and X-rays, it is not as easy to direct the beam as it is with electrons or ions. In both cases, the experimental method involves measuring the intensity of the scattered beam as a function of scattering angle.

TABLE 10.8 Properties of X-rays and Neutrons

Property	X-ray	Neutron
Wavelength	0.05–0.25 nm	0.01–2 nm
Energy	12.4 keV	80 MeV
Velocity	$3 \times 10^8\text{ m/s}$	$4 \times 10^3\text{ m/s}$
Production	X-ray tube Synchrotron	Nuclear reactor Electron linear accelerator pulsed source Proton spallation pulsed source
Detection	Photographic film Proportional counter Scintillation counter	$^{10}\text{BF}_3$ or ^3He proportional counter ^6Li scintillation counter

The obvious question is: Why use them when other particles do interact strongly? Neutrons offer distinct advantages over X-rays and other probes. They have a magnetic moment so they can detect magnetic ordering. Because they do not interact strongly they can be used to obtain bulk information. A major application is residual stress measurement in materials as a function of depth.

Neutrons have been used to study glasses and show a first sharp diffraction peak at low angles. This implies that there is some ordering in the glass. Intentional patterns of voids in glasses give rise to such peaks. Table 10.9 provides a comparison of the parameters for XRD and neutron diffraction.

Neutrons are produced in several ways, but each way requires a reactor. Thus neutron diffraction facilities are generally national facilities. In the United States there are seven centers for neutron scattering and there are about 30 in the world. A schematic of a neutron diffractometer is shown in Figure 10.32.

TABLE 10.9 Scattering of X-rays and Neutrons

Dependence	X-ray	Neutron
Nonmagnetic atom	Electrons scatter	Nucleus scatters
θ dependence	Depends on θ through $f(\theta)$	Depends on isotropic scattering length \bar{b}
Variation with Z	$F(0) = Z$	\bar{b} varies with Z
Phase change on scattering	π	Not always π
Isotope dependence	None	\bar{b} depends on isotope
Anomalous dispersion	Near an absorption edge	Near an absorption resonance
Magnetic atom	Nothing extra	Additional scattering (depends on θ)
Absorption coefficient	Absorption large	Absorption usually small

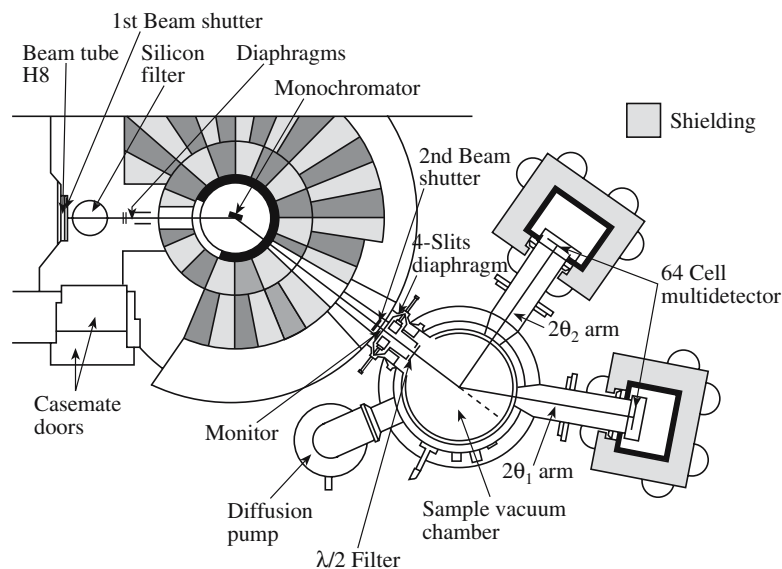


FIGURE 10.32 Schematic of a neutron scattering workstation. The width of the view is 10s of meters.

10.16 MASS SPECTROMETRY

Mass spectrometry is used to provide qualitative and quantitative chemical analysis. For ceramics we are mainly interested in analyzing solids, so a method for ionizing the material is necessary. In spark source mass spectrometry (SSMS) we use a high-voltage spark in a vacuum. The positive ions that are produced are analyzed by the spectrometer based on their mass. For insulating ceramics the material must be mixed with a conducting powder such as graphite or silver. Other methods can be used to ionize the sample:

1. Laser ionization MS uses an Nd:YAG laser and is ideal for insulators, but is qualitative more than quantitative because of the absence of standards.

2. Glow discharge ion source uses a gas discharge between two electrodes, so the sample must be conductive and formed into the cathode.

3. In secondary ion mass spectroscopy (SIMS) an incident ion beam with energy in the range of 4–15 keV is used to create secondary ions from the sample. This provides high-resolution depth profiles with a detection limit down to 1 ppb.

Secondary ion mass spectroscopy is like SEM, but it uses (usually Ga⁺) ions instead of electrons. Since the ions have more energy, they eject near-surface atoms out of the sample; these are collected and the chemistry of the near-surface area is thus determined. By scanning the ion beam we can generate a chemical image of the surface and by repeating this process (each time ejecting the surface atoms) we can generate a 3D profile of the sample.

10.17 SPECTROMETRY IN THE EM

The chemistry of interfaces can be probed using both XEDS and parallel recording of electron energy-loss spectra (PEELS).

In the earliest studies of solid-state reactions between ceramic oxides, the width of the reaction product produced by bulk diffusion couples was determined by VLM. Using an SEM with a field-emission gun a much more precise EDS profile analysis can be performed providing chemical analysis at a spatial resolution of ~2 nm. Figure 10.33 shows a typical XEDS spectrum: a plot of counts versus X-ray energy. The X-rays are produced as a result of electron transitions within the atoms in the sample. The transitions and, hence, the peaks are characteristic of specific atoms. A doped silicon crystal is used to detect the X-rays, where they cause the formation of electron-hole pairs. New methods for detecting the X-rays are being developed that use the change in temperature caused by the X-ray and are known as calorimeters.

The electron microprobe or WDS can provide accurate chemical analysis or a chemical profile across the interface. The wavelength of the X-rays emitted when the electron beam interacts with the sample is measured. Wavelength dispersive spectroscopy is more accurate than XEDS, but is a serial acquisition, so it is slower. Table 10.10 compares WDS and XEDS.

Electron energy-loss spectroscopy (EELS) counts the number of electrons that have lost particular quantities of energy when the incident electron beam passed through the TEM specimen. The energy loss can occur by interactions with different components of the structure (phonons and plasmons) or by the beam exciting core electrons to a different energy state. The EELS spectrum thus contains

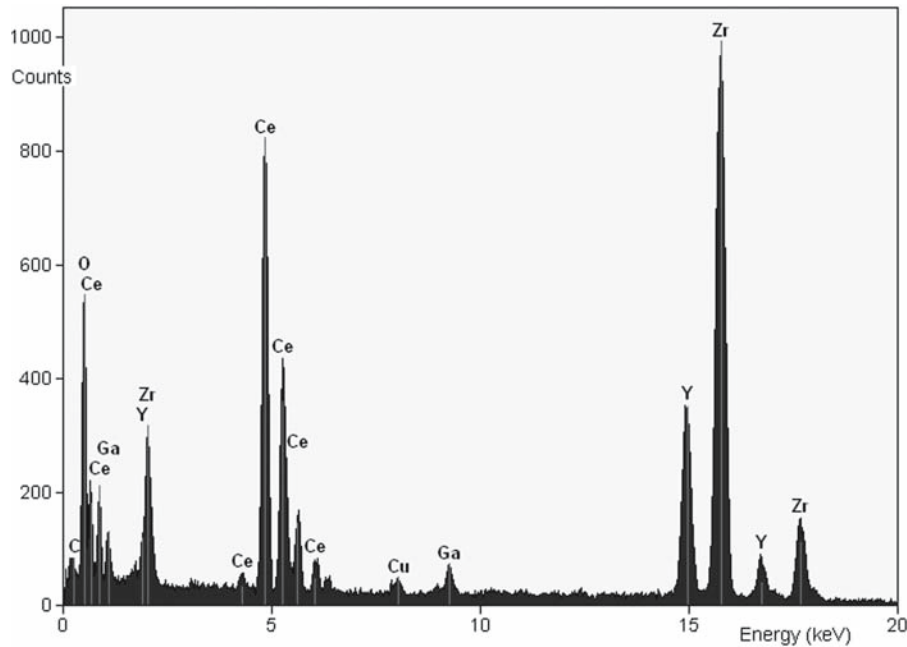


FIGURE 10.33 Example of an XEDS from a sample containing CeO₂ and YSZ in the range up to 20 keV.

information on the bonding and chemistry of the specimen. Since the beam in the TEM can now be as narrow as 0.1 nm, EELS can give highly localized information; it is particularly important in ceramics where low-Z elements tend to be particularly important. Figure 10.34 shows part of an EELS spectrum from two commercial ceria abrasives.

The fine structure of the EELS can be compared to the fine structure in X-ray scattering. It can be used in purpose-built chambers or, more recently, in the TEM. In the TEM you have the great advantage of knowing where you are getting the spectrum from—it is site specific. The difficulty with TEM, as usual, is that there are usually two surfaces to consider (you can try REELS—see REM). This technique will be used more in the future with the wider availability of TEM guns with a smaller spread in

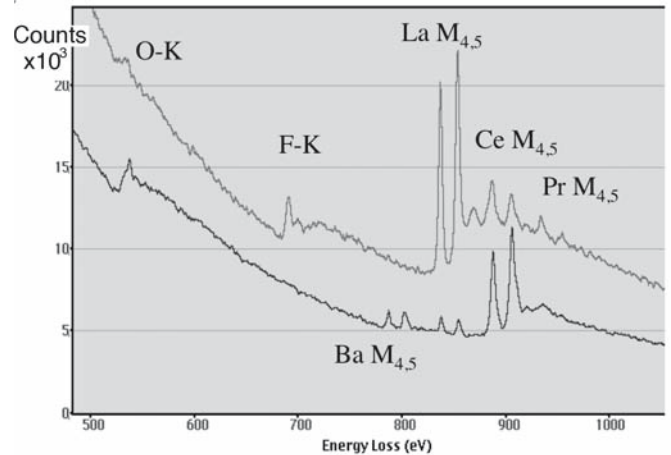


FIGURE 10.34 Example of EELS from two commercial ceria powders.

TABLE 10.10 Comparison of WDS and XEDS

Factor	WDS	XEDS	Reason for difference
Time for complete spectrum (minutes)	25–100	0.5–5	Collection efficiency XEDS measures whole spectrum simultaneously
Count rate on one peak (cps/nA)	1,000	10,000	Collection efficiency
Peak/background ratio	1,000	50	XEDS collects spurious X-rays and has high inherent noise
Maximum count rate (cps)	100,000	30,000	XEDS counts all channels simultaneously, and saturates
Resolution, 0.1–10 keV (eV)	5–10	150–200 80–100	Currently possible Theoretical limit; WDS inferior to XEDS above 25 keV (suitable crystals not available)
Detector limits (weight ppm)	50–1,000	2,000–5,000	WDS used at higher beam current, fewer overlapping peaks XEDS better if current is restricted, e.g., to avoid beam damage
Accuracy of analysis (%)	±1–2	±6	Experimentally determined
Light element analysis (min. atomic number)	4	4	Both have ability for light element detection providing windowless or polymer window used
Rough surface work	Bad	Good	XEDS insensitive to source position

energy. A major application for EELS, which we have only recently begun to use, is the direct measurement of bonding.

AUGER NOTATION

KVV refers to the series of electron transitions responsible for the Auger electron. V refers to electrons coming from the valence band of a solid.

10.18 ELECTRON SPECTROSCOPY

In the group of techniques known as photoelectron spectroscopy (PES) electrons are emitted from their filled electronic states in the solid by the absorption of single photons. Traditionally the energy of the photons corresponds to the UV or X-ray wavelengths and the techniques are known as ultraviolet photoelectron spectroscopy (UPS) or X-ray photoelectron spectroscopy (XPS). X-ray photoelectron spectroscopy used to be called electron spectroscopy for chemical analysis or ESCA and is still the most used surface-sensitive technique. The difficulty for ceramics is the usual one—as we remove electrons from the sample, the sample becomes charged and attracts the same electrons, which can distort the results. In principle you could use a flood gun to resupply the electrons, but the challenge is getting the balance right. The techniques do explore the surface region, not just the surface, so the surface effect must be separated from the larger bulk effect. Variations of the technique include angle-resolved photoemission spectroscopy (ARPES).

These techniques are mainly used for quantitative chemical analysis of surfaces by detecting electrons emitted from the surface. They can be differentiated by how the electrons are produced. In Auger electron spectroscopy (AES) the incident species are electrons. In XPS and UPS the incident species are photons. In XPS we illuminate the sample with X-rays and measure the energy of electrons that are then emitted. If the electrons come from regions close to the surface, we can obtain data on the chemistry and bonding close to the surface. The X-rays can be generated in a synchrotron and this will have both high spatial resolution and high intensity.

Auger electrons are created when an incident electron beam ionizes an atom by removing an inner-shell electron. An electron from a higher energy level will fill the hole and the resulting kinetic energy will be transferred to a loosely bound electron, which is detected. These Auger electrons have relatively low kinetic energy and, consequently, a short mean free path. They come from the top 0.5–3 nm of the surface. Their energy is characteristic of the atomic energy levels of the atom from which they came. Therefore, they are sensitive surface probes of chemical composition. Auger electron spectroscopy has been used extensively to study oxide surfaces. The problem is that the surface must be very clean and examined in UHV.

Figure 10.35 shows examples of carbon KVV Auger electron spectra generated from the surface of two different carbides, diamond and graphite. The

spectra are in the form of derivative electron yield versus electron energy and show the chemical shift effect and how this could be used for “fingerprinting” an unknown sample. Auger electron spectroscopy is the spectroscopist’s variation of low-energy electron diffraction (LEED). Its main use is to provide information on the chemistry, rather than bonding, and more specifically to determine if the sample is clean enough for LEED. The beam can be scanned across the sample to produce an image, hence scanning Auger microscopy (SAM).

In XPS electrons with binding energy (E_b) are ejected from core levels by an incident X-ray photon with energy E_0 . The ejected photoelectron has energy ($E_0 - E_b$). Output electron energies are typically >10 eV. X-ray photon spectroscopy, like AES, has excellent depth resolution and is sensitive to the near surface region of a material. The spectrum has the form of intensity versus binding energy.

By sputtering the surface in between acquisition of either an AES or XPS spectrum it is possible to obtain depth profiles. Sputtering must be conducted in the same system as the spectrometer to avoid contamination of the

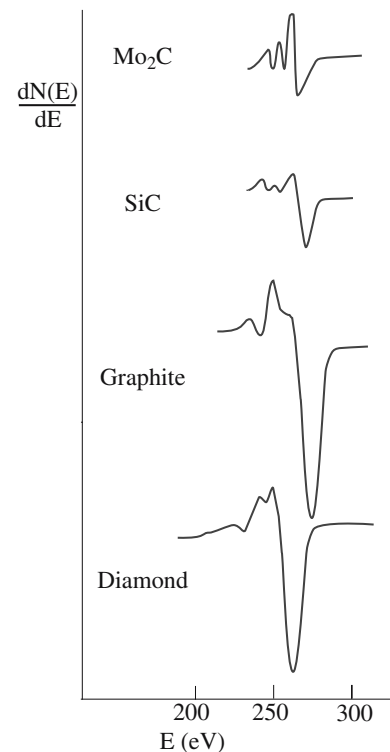


FIGURE 10.35 Derivative C KVV Auger electron spectra from two carbides, graphite, and diamond.

surface. Ultraviolet photoelectron spectroscopy uses UV light to produce electrons. Using these lower photon energies (typically ~ 21 eV) only the valence levels are accessible. A major application of UPS is in determining the band structure of solid surfaces.

10.19 NEUTRON ACTIVATION ANALYSIS (NAA)

The basis of neutron activation analysis is that if a material containing certain rare earth elements is exposed to a beam of neutrons it can become highly radioactive. If the induced radioactivity is then measured, it is possible to identify the elements that are present in the samples and quantify the amount present. The neutron interacts with the target nucleus and forms an excited nucleus, i.e., the neutron loses energy. The excited nucleus then quickly relaxes back to a more stable state by emitting a characteristic γ -ray (this is an n,γ nuclear reaction). The new nucleus may be radioactive, in which case it will then begin to decay by emitting additional characteristic γ -rays, but the rate of emission will be slower due to the longer half-life of the decaying nucleus. Figure 10.36 gives a schematic of the NAA process.

The quick emission of the γ -ray produces the PGNAA (prompt γ -ray NAA) technique and the slower emission produces the more usual DGNAA (delayed GNAA but often just called NAA) technique. Of the three principal different types of neutron sources (reactors, accelerators, and radioisotope neutron emitters), nuclear reactors generating neutrons by U fission give particularly high fluxes of neutrons. Thermal neutrons have energies < 0.5 eV; if the neutrons are in thermal equilibrium with the moderator of the reactor, they have a mean energy of 25 meV, which means they have a velocity of 2.2 km s^{-1} . A 1-MW reactor will have a peak flux of thermal neutrons of $\sim 10^{13} \text{ cm}^{-2} \text{ s}^{-1}$. Table 10.11 shows how sensitive NAA is for detecting elements in a sample.

As an example of an analysis, crush a sample to a fine powder and put 150 mg in a plastic vial and 200 mg in a high-purity quartz capsule. Reference samples of known composition are also prepared. The plastic vial is given a

TABLE 10.11 The Sensitivity for Detecting Elements by NAA

(Sensitivity ng)	Elements
0.1	Dy, Eu
0.1–1	In, Lu, Mn
1–10	Au, Ho, Ir, Re, Sm, W
10–100	Ag, Ar, As, Br, Cl, Co, Cs, Cu, Er, Ga, Hf, I, La, Sb, Sc, Se, Ta, Tb, Th, Tm, U, V, Yb
100–1,000	Al, Ba, Cd, Ce, Cr, Hg, Kr, Gd, Ge, Mo, Na, Nd, Ni, Os, Pd, Rb, Rh, Ru, Sr, Te, Zn, Zr
1,000–10,000	Bi, Ca, K, Mg, P, Pt, Si, Sn, Ti, Tl, Xe, Y
10,000–100,000	F, Fe, Nb, Ne
1000,000	Pb, S

5-second irradiation with a flux of 8×10^{13} neutrons $\text{cm}^{-2} \text{ s}^{-1}$. The γ -rays are then counted for 720 seconds, which gives a γ -spectrum (PGNAA) for short-lived elements (Al, Ba, Ca, Dy, K, Mn, Na, Ti, V). The samples in quartz are irradiated for 24 hours with a flux of 5×10^{13} neutrons $\text{cm}^{-2} \text{ s}^{-1}$. After leaving the sample for 7 days, the γ -rays are counted for 2000 seconds. This middle count gives medium half-life elements As, La, Lu, Ne, Sm, U, and Y. After a further 4 weeks, the final count (9000 seconds) give a measure of the long half-life elements Ce, Co, Cr, Cs, Eu, Fe, Hf, Ni, Rub, Sb, Sc, Sr, Ta, Tb, Th, Zn, and Zr. The results are then compared to those from the known material. The accuracy can be better than parts per billion.

Applications have included identifying the origin of archeological ceramics: obsidian can be fingerprinted and the trade patterns of the Olmec civilization can be followed by identifying the area from which the clay they used in their pots originated and the source of contamination in semiconductors can be traced at the 1 ppb level.

10.20 THERMAL ANALYSIS

The term “thermal analysis” actually covers many different techniques that measure a change in a material as a function of temperature. Thermal analysis is particularly useful in characterizing decomposition and crystallization during ceramic powder processing. It is then possible to

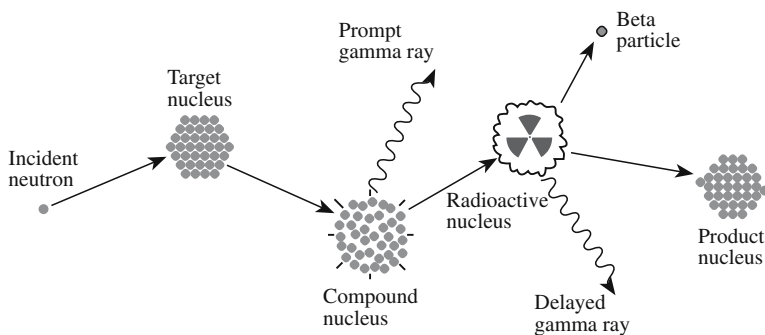


FIGURE 10.36 Schematic of the NAA process.

TABLE 10.12 Common Thermoanalytical Techniques

Method	Common abbreviation	Property measured
Thermogravimetry	TG (TGA)	Mass
Differential thermal analysis	DTA	ΔT between sample and reference
Differential scanning calorimetry	DSC	Heat absorbed or evolved by sample
Evolved gas analysis	EGA	Nature and amount of evolved gas species
Thermodilatometry	TD	Dimension
Thermomechanical analysis	TMA	Deformation/nonoscillatory load
Dynamic thermomechanometry	DMA	Deformation/oscillatory load
Thermomagnetometry	TM	Relative magnetic susceptibility

determine optimum calcination temperatures. A list of the main thermal analysis techniques is given in Table 10.12. The two most common are

- Thermogravimetric analysis (TGA), which measures weight loss during heating
- Differential thermal analysis (DTA), which measures relative changes in sample temperature during heating

DTA and TGA can be performed separately or simultaneously. Figure 10.37 shows examples of DTA and TGA analysis on an initially amorphous CA_2 powder as it crystallizes. The TGA plot shows that as temperature is

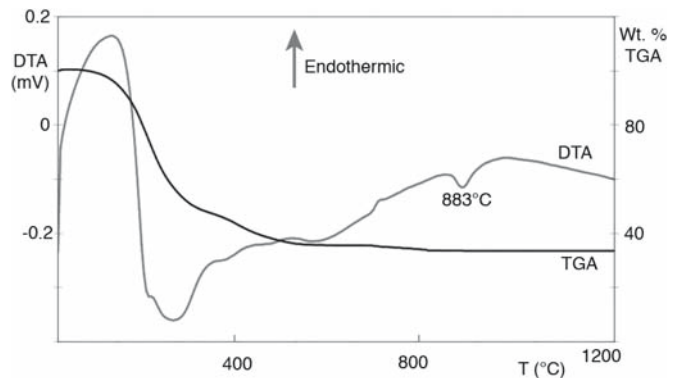


FIGURE 10.37 DTA and TGA measurements showing the reaction as CA_2 crystallizes.

increased the sample loses weight and by about 600°C weight loss is complete. The DTA plot shows that the CA_2 crystallization is exothermic.

Thermal analysis techniques are widely used to study ceramic processing. In addition to determining decomposition and crystallization processes it is also possible to monitor the burnout of organic binders, which are commonly added to powders prior to shaping, and shrinkage during drying. One of the earliest uses for DTA was in studying clay minerals. In montmorillonite the position of certain cations can have an influence on the dehydration behavior. Analysis of DTA curves from samples of montmorillonite containing Li, Na, or K shows that the presence of Li stabilizes the water of hydration and higher temperatures are required for dehydration.

CHAPTER SUMMARY

There are many different techniques for studying ceramics. The choice of which one to use depends on the type of information that we want to obtain and how valuable our material is. Transmission electron microscopy is destructive, but so are many other methods if we have to produce a fine powder. Whereas some of the techniques we described, such as VLM and SEM, are universal, there are many techniques that are available in only a few sites. Those requiring nuclear reactors or very high flux photon beams are usually found at National User Facilities.

A full understanding of a material or a process may require the use of several complementary techniques. For example, electron diffraction in the TEM combined with FTIR and Raman spectroscopies can unequivocally determine what polymorph of SiO_2 is present in a sample. For example, AES can give us the composition of the surface of a sample, AFM can give us the surface morphology, and RHEED can give us the surface crystallography.

The technological importance of nanomaterials means that we need high-resolution techniques. It is the need to understand the structure of nanomaterials and processes that happen on atomic and molecular levels that leads to the development of new instrumentation for characterizing materials.

PEOPLE IN HISTORY

Binnig, Gerd (1947–) and Heinrich Rohrer (1933–) of the IBM Research Laboratory in Switzerland won the Nobel Prize in Physics in 1986 for their invention of the STM.

Mössbauer, Rudolf (1929–) received the Nobel Prize in Physics in 1961 for the discovery of the Mössbauer effect.

Raman, Sir Chandrasekhara Venkata (1888–1970), the Indian scientist, discovered the phenomenon in 1928 while studying CCl_4 ; he was awarded the Nobel Prize in Physics in 1930.

Rutherford, Ernest (1871–1937) demonstrated ion scattering and its utility for chemical analysis. He won the 1908 Nobel Prize in Chemistry.

Stokes, George Gabriel, born 13 August 1819, died 1 February 1903, was Professor of Mathematics in Cambridge when Rayleigh was an undergraduate.

Strutt, John William (Lord Rayleigh) was born 12 November 1842 and died 30 June 1919. He won the Nobel Prize in Physics in 1904 for discovering Ar and succeeded James Clerk Maxwell as the Cavendish Professor in Cambridge.

GENERAL REFERENCES

Cahn, R.W. (2005) *Concise Encyclopedia of Materials Characterization*, 2nd edition, Elsevier, Amsterdam, The Netherlands. A good place to check out any technique.

Chu, W.K., Mayer, J.W. and Nicolet, M-A. (1978) *Backscattering Spectrometry*, Academic Press, New York. Detailed information about RBS.

Hartshorne, N.H. and Stuart, A. (1970) *Crystals and the Polarizing Microscope*, 4th edition, Arnold, London.

Hollas, J.M. (2004) *Modern Spectroscopy*, 4th edition, Wiley, Chichester, England. Covers a wide range of topics at the level you will need if you use the techniques.

Loehman, R.E. (Ed.) (1993) *Characterization of Ceramics*, Butterworth-Heinemann, Boston. Provides “case studies” in which various techniques are used.

Wachtman, J.B. (1993) *Characterization of Materials*, Butterworth-Heinemann, Boston. Overview and comparison of the different characterization techniques.

SPECIFIC REFERENCES

Binnig, G., Rohrer, H., Gerber, Ch., and Weibel, E. (1982) “Tunneling through a controllable vacuum gap,” *Appl. Phys. Lett.* **40**, 178. Paper describing the STM.

Blanpain, B., Revesz, P., Doolittle, L.R., Purser, K.H., and Mayer, J.W. (1988) “The use of the 3.05 MeV oxygen resonance for He-4 backscattering near-surface analysis of oxygen-containing high Z compounds,” *Nucl. Instrum. Methods* **B34**, 459. Describes the RBS method used to obtain the enhanced oxygen signal.

Philp, E., Sloan, J., Kirkland, A.I., Meyer, R.R., Friedrichs, S., Hutchison, J.L., and Green, M.L.H. (2003) “An encapsulated helical one-dimensional cobalt iodide nanostructure,” *Nature Materials* **2**, 788.

Raman, C.V. and Krishnan, K.S. (1928) “A new type of secondary radiation,” *Nature* **121**, 501. The original description of the “Raman effect.”

“Standard Test Method for Interstitial Atomic Oxygen Content of Silicon by Infrared Absorption,” F 121 *Annual Book of ASTM Standards*, Vol. 10.05, ASTM, Philadelphia, pp. 240–242.

EXERCISES

- 10.1 Construct a chart summarizing the principal scattering techniques used to characterize the structure, chemistry, and bonding in ceramics emphasizing which of the three features is most directly addressed by each technique.
- 10.2 In Figure 10.1 the grains boundaries are described as low-angle grain boundaries. Could this information be obtained directly from VLM? If not, what other methods might have been used to make this determination?
- 10.3 In Figure 10.6, why does the image have a 3D appearance?
- 10.4 In Figure 10.7 the image distinguishes the regions with different chemistry directly and with high spatial resolution. Explain the physical process underlying this observation?
- 10.5 During the processing of ceramics containing crystalline quartz a phase transformation occurs on cooling/heating between the α form and the β form. The phase transformation produces an appreciable change in volume that can lead to cracking. How would you determine from a fragment of a ceramic plate whether you had the α or β phase present in the sample?
- 10.6 How would you determine whether water vapor has chemisorbed onto the surface of particles of silica gel?
- 10.7 If we are examining steps of atomic dimensions in figure 10.14, redraw the schematic to scale and thus explain the factors that determine vertical and lateral resolution in AFM.
- 10.8 Compare the value of NMR and Mössbauer analysis for ceramic materials.
- 10.9 Referring to Figure 10.33, explain why we see multiple peaks for Y and Zn occur at different energies, and why we see Cu.
- 10.10 Examine the DTA/TGA plots in Figure 10.37. What can you say about the curves as the temperature is increased from 25°C to 1200°C?